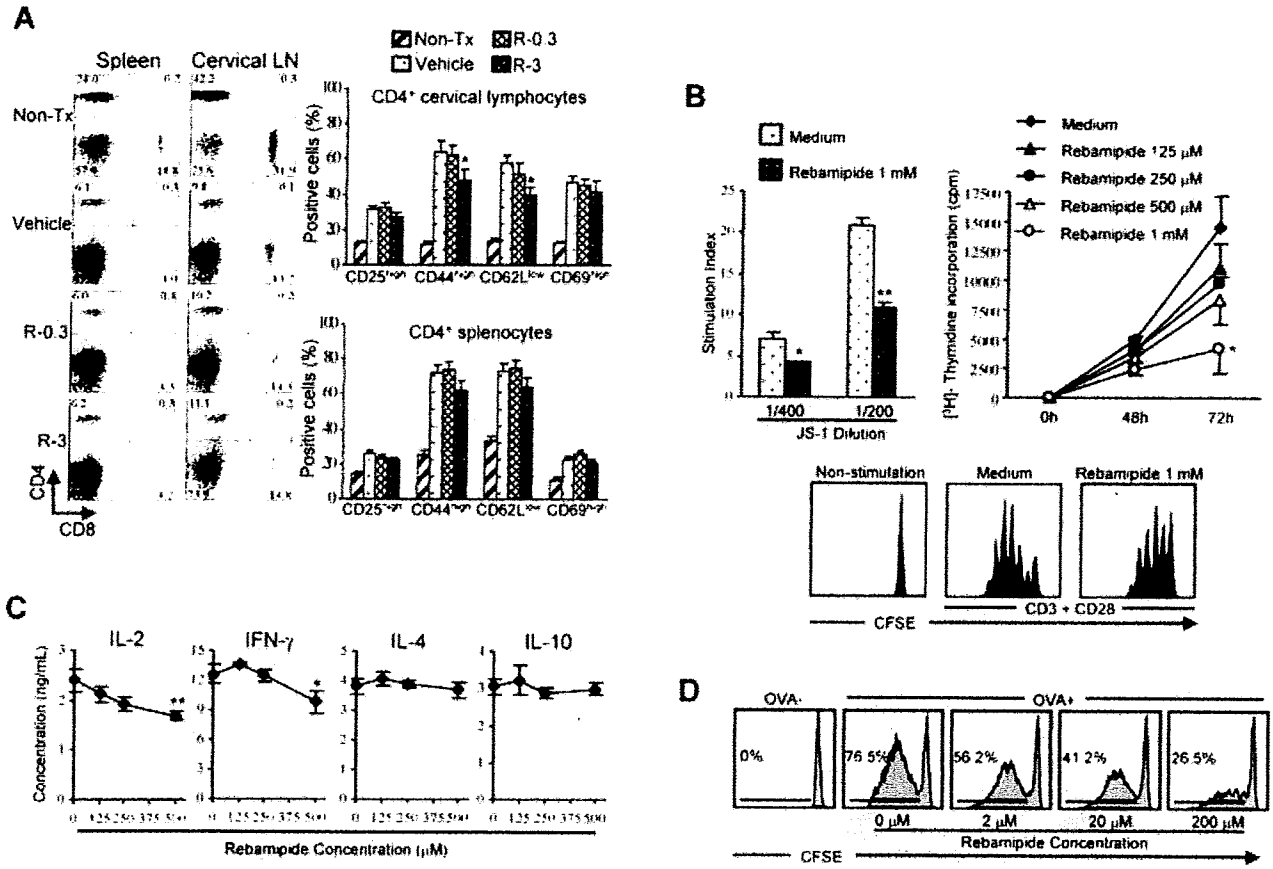

Figure 3. Effect of rebamipide on T cell phenotypes and functions in the NFS/*sld* mouse model of Sjögren's syndrome. Mice underwent thymectomy on day 3 after birth and were treated with vehicle, 0.3 mg/kg of rebamipide (R-0.3), or 3 mg/kg of rebamipide (R-3) from age 4 weeks to age 8 weeks. A group of nonthymectomized (non-Tx), vehicle-treated mice was also studied. **A,** CD4+ and CD8+ T cell subsets in the spleen and cervical lymph nodes of the 4 groups of mice, as analyzed by flow cytometry (left). Numbers shown in each compartment are the percentage of positive cells. Results are representative of 10 mice per group. Memory markers on CD4+ T cells derived from the cervical lymph nodes and spleen of the 4 groups of mice were also analyzed by flow cytometry (right). Values are the mean and SEM of 10 mice per group. **B,** Antigen-specific and nonspecific T cell responses. Purified CD4+ T cells from the spleen of thymectomized mice were cultured for 72 hours with irradiated T cell–depleted splenocytes in the presence of recombinant α-fodrin (JS-1), with and without rebamipide (top left). Values are the mean and SEM. * = $P < 0.05$; ** = $P < 0.01$ versus medium alone, by Dunnett's test. Incorporation of ^{3}H-thymidine into purified CD4+ T cells stimulated with anti-CD3 and anti-CD28 monoclonal antibodies (mAb) and treated for 48 or 72 hours with the indicated concentrations of rebamipide or medium alone was determined during the last 12 hours of culture (top right). Results are representative of 3 independent experiments. Values are the mean and SEM of triplicate wells. In addition, CD4+ T cells were labeled with carboxyfluorescein succinimidyl ester (CFSE) and were left unstimulated or were stimulated with anti-CD3 and anti-CD28 mAb for 72 hours in the presence of medium alone or 1 m*M* rebamipide (bottom). Cell division was analyzed by flow cytometry. * = $P < 0.01$ versus medium alone, by Dunnett's test. **C,** Production of interleukin-2 (IL-2), interferon-γ (IFNγ), IL-4, and IL-10 by CD4+ T cells stimulated for 72 hours with anti-CD3 and anti-CD28 mAb in the presence of medium alone or the indicated concentrations of rebamipide, as determined by enzyme-linked immunosorbent assay of culture supernatants. Results are representative of 3 independent experiments. Values are the mean ± SEM of triplicate samples. * = $P < 0.05$; ** = $P < 0.01$ versus medium alone, by Dunnett's test. **D,** Flow cytometry of CFSE-labeled CD4+ T cells (5×10^6) derived from transgenic OT-2 mice and transferred intravenously into B6 (Ly5.1+) mice. Ovalbumin (OVA) peptide (100 μg) was injected intraperitoneally, and rebamipide (0–200 μ*M*) was injected intravenously, into recipient mice. After 3 days, the CFSE dilution of Ly5.2+,V_β5.2+,CD4+ T cells was analyzed. Results are representative of 3–5 mice per group.

present study, we observed a decrease in TUNEL+ apoptotic epithelial cells in the salivary glands of mice treated with rebamipide as compared with those in vehicle-treated mice (Figures 2A and B). Indeed, expression of FasL and NF-κB genes on CD4+ T cells was significantly inhibited by rebamipide treatment (Figure 2C), possibly being consistent with the finding of decreased TUNEL+ epithelial cell apoptosis in the

Table 1. Autoantibody production in the NFS/*sld* mouse model of Sjögren's syndrome after treatment with rebamipide or vehicle alone*

Antibody	No. (%) of nonthymectomized, vehicle-treated mice (n = 10)	Treatment in thymectomized mice		
		No. (%) receiving vehicle (n = 12)	No. (%) receiving 0.3 mg/kg of rebamipide (n = 12)	No. (%) receiving 3 mg/kg of rebamipide (n = 11)
SSA/Ro	0 (0)	12 (100)	11 (92)	8 (73)†
SSB/La	0 (0)	11 (92)	10 (83)	6 (55)†
JS-1	0 (0)	7 (58)	4 (33)	4 (36)
ssDNA	0 (0)	11 (92)	12 (100)	7 (64)

* Mice were subjected to thymectomy on day 3 after birth. Autoantibodies were detected by enzyme-linked immunosorbent assay of sera obtained at the end of treatment (8 weeks of age). A positive result was defined as a value higher than the mean ± 3SD of the optical density value in nonthymectomized NFS/*sld* mice. JS-1 is an α-fodrin–specific antibody. ssDNA = single-stranded DNA.
† $P < 0.05$ versus vehicle-treated mice, by chi-square test.

rebamipide-treated mice. In addition, we confirmed the dose-dependent decrease in phosphorylation of IκB in CD4+ T cells from mice treated with rebamipide as compared with vehicle-treated controls (Figure 2D). Furthermore, nuclear translocation of NF-κB subunits (RelA and p65) in CD4+ T cells from rebamipide-treated mice had decreased remarkably compared with that in cells from vehicle-treated controls (Figure 2D).

Inhibitory effects of rebamipide on T cell activation. We next examined whether the therapeutic effect of oral administration of rebamipide on thymectomized NFS/*sld* mice was attributable to the inhibition of T cell activation. Cervical lymph node cells and spleen cells were purified from thymectomized NFS/*sld* mice treated with rebamipide or vehicle from ages 4 weeks to 8 weeks. In rebamipide-treated mice, the number of CD4+ and CD8+ T cells from the lymph node and spleen did not change with oral administration of rebamipide at either dose (Figure 3A).

We next examined CD25, CD44, CD62L, and CD69 expression on CD4+ T cells because these makers are known to be highly expressed on activated T cells and memory T cells (28). We found a decreased expression of CD4+,CD62L^{low} effector T cells in lymph nodes from mice treated with rebamipide, as compared with those from the control group (Figure 3A). In contrast, the expression of these markers on splenic CD4+ T cells from rebamipide-treated mice was similar to that in splenic CD4+ T cells from vehicle-treated controls (Figure 3A). It has recently been demonstrated that autoimmunity could be induced by specific in vivo expansion of CD4+,CD62L^{low} effector T cells (29).

Inhibitory effects of rebamipide on T cell proliferation and cytokine production. We previously reported that CD4+ T cells from thymectomized mice responded to the α-fodrin peptide JS-1 (25). Thus, we examined whether the rebamipide treatment affects the JS-1–specific proliferative response of splenic CD4+ T cells. A significant decrease in autoantigen (JS-1)–specific T cell proliferation was observed in CD4+ T cells treated with rebamipide (Figure 3B, top left). These results suggest that rebamipide treatment reduced the expansion of JS-1–specific T cells in mice, which is consistent with the low levels of CD4+,CD62L^{low} effector T cells in the rebamipide-treated mice. The proliferative response of anti-CD3 and anti-CD28 mAb-stimulated CD4+ T cells was also decreased by the addition of rebamipide in a dose-dependent manner (Figure 3B, top right). Furthermore, when CFSE-labeled CD4+ T cells were stimulated with anti-CD3 and anti-CD28 mAb in the presence of rebamipide for 72 hours, cell division was suppressed by rebamipide (Figure 3B, bottom).

To confirm the inhibitory effect of rebamipide, an in vitro cytokine assay was performed using splenic CD4+ T cells stimulated with anti-CD3 and anti-CD28. We obtained clear evidence that rebamipide treatment inhibited the production of Th1 (IL-2 and IFNγ), but not Th2 (IL-4 and IL-10), cytokines (Figure 3C). In serum samples, we detected no IL-2, IL-4, or IFNγ in mice treated with rebamipide (data not shown).

It was still unclear whether the antigen-specific T cell response in a normal mouse strain is inhibited by rebamipide. Therefore, CFSE-labeled T cells from OT-2 mice transgenic for ovalbumin-specific T cell receptor

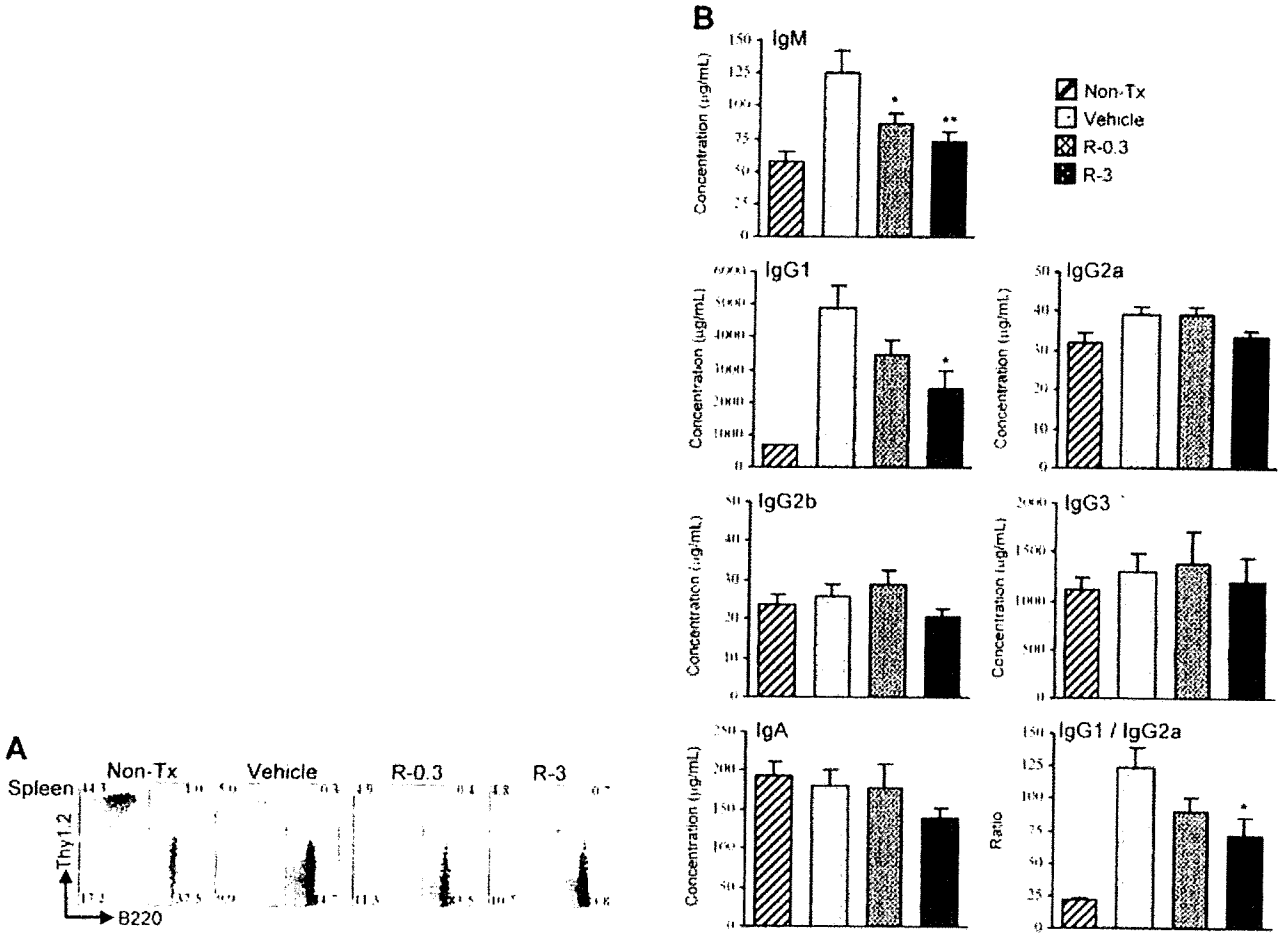

Figure 4. Effect of rebamipide on B cell function in the NFS/*sld* mouse model of Sjögren's syndrome after treatment with rebamipide. Mice underwent thymectomy on day 3 after birth and were treated with vehicle, 0.3 mg/kg of rebamipide (R-0.3), or 3 mg/kg of rebamipide (R-3) from age 4 weeks to age 8 weeks. A group of nonthymectomized (non-Tx), vehicle-treated mice was also studied. **A,** Thy1.2+ and B220+ cell subsets in the spleen of the 4 groups of mice, as determined by flow cytometry. Numbers shown in each compartment are the percentage of positive cells. Results are representative of 10–12 mice per group. **B,** Serum concentrations of immunoglobulin subclasses in the 4 groups of mice, as determined by enzyme-linked immunosorbent assay. Values are the mean and SEM of 10 mice per group. * = $P < 0.05$; ** = $P < 0.01$ versus the vehicle-treated group, by Dunnett's test.

were transferred into B6 (Ly5.1+) mice, and ovalbumin peptide was injected into the mice together with rebamipide. Treatment with rebamipide resulted in a dose-dependent inhibition of ovalbumin-specific T cell expansion in vivo (Figure 3D).

Reduced serum autoantibody production with rebamipide treatment. Sera were collected after rebamipide and vehicle treatment to evaluate the production of autoantibodies. Thymectomized NFS/*sld* mice have high titers of serum autoantibody against recombinant α-fodrin protein (JS-1) (25). We examined whether oral administration of rebamipide affected serum levels of autoantibody against α-fodrin in this mouse model of SS. As shown in Table 1, the titer of autoantibody against α-fodrin (JS-1) was considerably lower in mice treated with rebamipide than in mice treated with vehicle. The decreased serum titer of autoantibody against α-fodrin suggests that oral administration of rebamipide affected the autoimmune pathology and was able to suppress the systemic production of α-fodrin–specific autoantibody. We also examined serum titers of autoantibodies that are often associated with SS: anti-SSA/Ro, anti-SSB/La, anti-ssDNA, and anti–α-fodrin (30–33). Serum titers of anti-SSA/Ro and anti-SSB/La autoantibodies were significantly decreased in mice treated with rebamipide, but titers of anti–α-fodrin were not statistically significantly different from those in the control mice (Table 1).

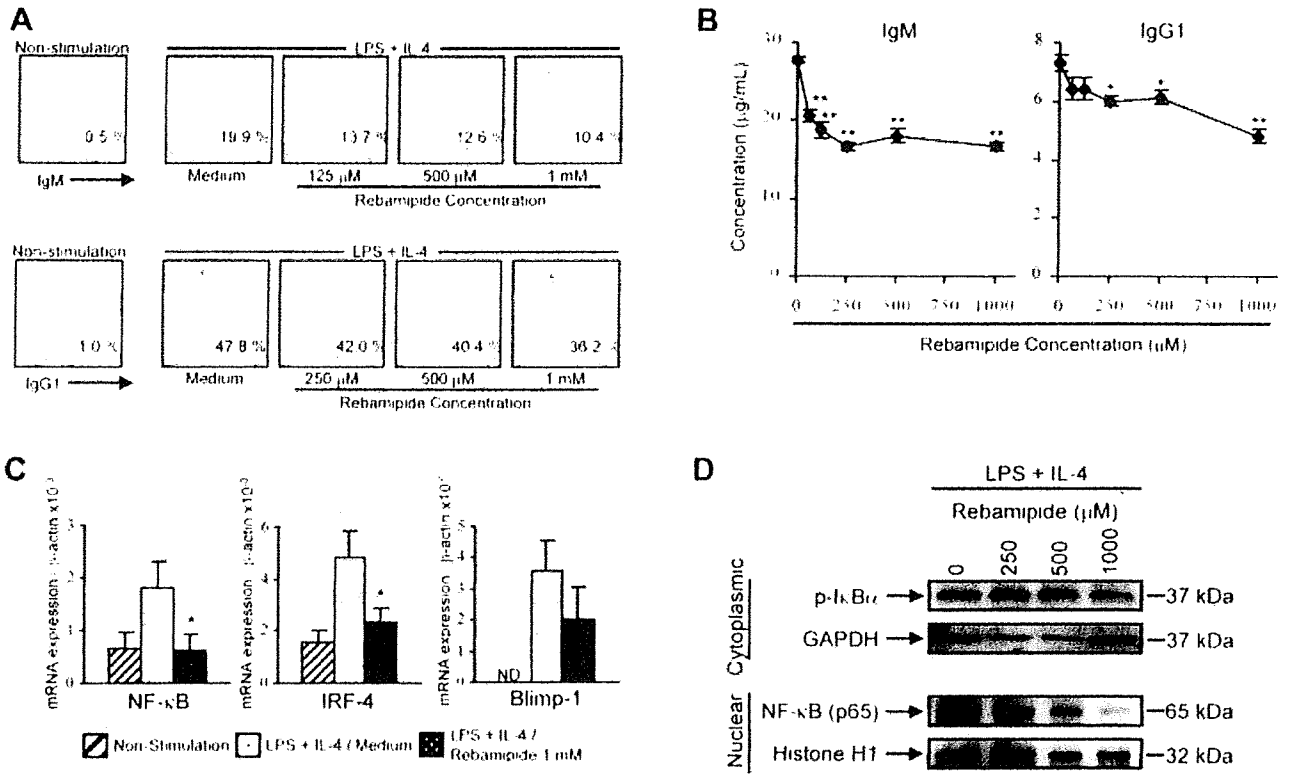

Figure 5. Effect of rebamipide on immunoglobulin production in the NFS/*sld* mouse model of Sjögren's syndrome. Mice underwent thymectomy on day 3 after birth and were treated with 3 mg/kg of rebamipide from age 4 weeks to age 8 weeks. **A,** Cell surface expression of IgM and IgG1, as detected by flow cytometry. Enriched splenic B cells were left unstimulated or were stimulated with lipopolysaccharide (LPS) and interleukin-4 (IL-4) in the presence of the indicated concentrations of rebamipide for 5 days. Values are the percentage of positive cells. **B,** Secretion of IgM and IgG1 into supernatants from B cells stimulated for 5 days with LPS and IL-4 in the presence of the indicated concentrations of rebamipide, as detected by enzyme-linked immunosorbent assay. Values are the mean ± SEM of 10 mice. * = $P < 0.05$; ** = $P < 0.01$ versus medium alone, by Dunnett's test. **C,** Expression of mRNA for NF-κB, interferon regulatory factor 4 (IRF-4), and B lymphocyte–induced maturation protein 1 (BLIMP-1), by stimulated B cells, as determined by quantitative reverse transcription–polymerase chain reaction analysis. Results are representative of 3 independent experiments. Values are the mean and SEM expression relative to β-actin mRNA in triplicate wells. * = $P < 0.05$ versus medium alone, by Student's *t*-test. ND = not detected. **D,** Phosphorylation of IκB and nuclear translocation of NF-κB in cytoplasmic and nuclear extracts of activated B cells treated with LPS and IL-4 in the presence of rebamipide, as analyzed by Western blotting. GAPDH and histone H1 were use as the respective internal controls. Results are representative of 3 independent experiments.

Reduced serum immunoglobulin levels with rebamipide treatment. In rebamipide-treated mice, the number of splenic B220+ B cells did not change with oral administration of either dose of rebamipide (Figure 4A). We found that thymectomized NFS/*sld* mice developed hypergammaglobulinemia involving both IgG1 and IgM as compared with nonthymectomized control mice (Figure 4B). Rebamipide-treated mice showed prominent inhibition of serum IgM and IgG1 levels ($P < 0.01$), but not the other IgG subclasses or IgA (Figure 4B). This may indicate that oral administration of rebamipide affected all B cell function, which was able to suppress systemic secretion of IgM and IgG1.

Inhibitory effects of rebamipide on immunoglobulin secretion. To confirm the inhibitory effects of rebamipide on IgM and IgG1 secretion, we examined the effects of in vitro treatment with rebamipide using splenic B220+ B cells stimulated with LPS and IL-4. We found that rebamipide inhibited B cell production of IgM and IgG1, as determined by flow cytometry (Figure 5A). Rebamipide also inhibited IgM and IgG1 in culture supernatants, as determined by ELISA (Figure 5B). Both of these effects were dose-dependent. Since rebamipide treatment in this mouse model of SS inhibited the production of autoantibodies and immunoglobulins, we also examined the transcriptional activity of NF-κB,

IRF-4, and BLIMP-1. Significant inhibitory effects of rebamipide on the expression of mRNA for NF-κB and IRF-4, transcription factors that are associated with B cell activation and differentiation, were observed (Figure 5C). We confirmed the dose-dependent decrease in phospho-IκB and NF-κB subunits (p65) in activated B cells stimulated with LPS and IL-4 as compared with vehicle-treated controls (Figure 5D).

DISCUSSION

Since studies of animal models of autoimmune disorders should eventually give rise to appropriate potential treatments in humans with those diseases, it is important to identify the best therapeutic approach by which cells of the immune system can be specifically affected without causing side effects. In this regard, antigen-specific down-regulation of autoimmune processes is considered to be the most suitable therapy (34–36). The findings of the present study of rebamipide treatment in the NFS/*sld* mouse model of Sjögren's syndrome confirm the protective effect of rebamipide on the functional recovery of T cells and B cells in this autoimmune exocrinopathy, probably based on its capacity to inhibit T cell activation and B cell proliferation, in addition to reinforcing the epithelial barrier. Although therapy in SS patients has generally consisted of systemic administration of immunosuppressive or antimuscarinic drugs, it has been known that the systemic use of these drugs induces severe side effects (34). In contrast, it has been reported that oral administration of rebamipide had no clinically significant physical side effects, with normal blood pressure and pulse rate, in healthy adult subjects (37). This study is the first to demonstrate that oral administration of rebamipide effectively inhibits autoimmune pathology in the NFS/*sld* mouse model of SS without causing systemic histopathologic changes.

We previously reported that a cleavage product of 120-kd α-fodrin may be an important autoantigen in the development of primary SS and that anti–120-kd α-fodrin antibodies have been frequently detected in sera from SS patients (25). We have also reported a significant increase in TUNEL+ apoptotic epithelial duct cells in the salivary glands of thymectomized NFS/*sld* mice and a large proportion of FasL in tissue-infiltrating CD4+ T cells (11); both findings support the idea that tissue-infiltrating CD4+ T cells are responsible for tissue destruction, as determined by in vitro cytotoxicity assay. Our data have suggested that one mechanism by which activated CD4+ T cells induce cytotoxicity to salivary gland cells in this murine model of SS is Fas-based and that the primary mediators of the disease are autoantigen-driven T cell responses. In the present study, we found that expression of FasL on CD4+ T cells was significantly inhibited and that TUNEL+ epithelial cell apoptosis declined in the rebamipide-treated mice. A significant decrease in autoantigen-specific T cell proliferation was observed in CD4+ T cells with rebamipide treatment. This is consistent with the finding that rebamipide treatment resulted in the dose-dependent inhibition of ovalbumin-specific T cell expansion in vivo.

In addition, we observed that rebamipide treatment induced a selective impairment of CD4+,CD62L^{low} effector T cells in the lymph nodes. This population was more potent than the population of CD4+,CD62L^{high} cells in inducing a self-directed immune response, as demonstrated by cytometric isolation and adoptive transfer experiments. The induction of autoimmunity by specific in vivo expansion of CD4+,CD62L^{low} cells has recently been demonstrated (29), indicating that CD4+,CD62L^{low} effector T cells may be attractive targets for immune interventions in the treatment of autoimmune diseases. On the other hand, rebamipide treatment did not influence the frequency of CD4+,CD25+ natural regulatory T cells in cervical lymph nodes (data not shown). It is noteworthy that rebamipide treatment inhibited T cell proliferation and Th1 cytokine production (IL-2 and IFNγ). These data indicate that rebamipide treatment effectively inhibits autoimmune pathology in the NFS/*sld* mouse model of SS.

The improvement in secretory function after treatment with rebamipide, as demonstrated by saliva volumes, strongly points to the ingestive mechanism of action of rebamipide. With regard to the small discrepancy between the histologic features of the lacrimal glands and the lacrimal gland function, as demonstrated by tear flow volumes after treatment of rebamipide (see Figure 1), it has been reported that inflammatory lesions in the lacrimal gland develop later than those in the salivary gland in our mouse model (22). It is also possible that the effects of rebamipide on salivary gland cells may be different from the effects on lacrimal gland cells.

The beneficial effects of rebamipide on the epithelial barrier, which have previously been demonstrated in the gastric and small intestinal mucosa (38,39), have possibly, although not definitively, also been shown for the salivary gland epithelia, although the findings are not definitive. While the mechanism of action of rebamipide

on epithelial permeability, which has mostly been studied in the stomach, is not completely understood, it could be related to the capacity of rebamipide to act as a scavenger of cytokine-induced hydroxyl radicals (40) or to induce prostaglandin production (41). Since we found decreased apoptosis of salivary gland epithelia in rebamipide-treated mice, it is possible that the protective effect of rebamipide on the salivary gland epithelia could also account for its beneficial effect on ulcerative colitis in humans or on Dextran sulfate sodium–induced colitis in rats (42). This improvement in the epithelial barrier, together with the capacity of rebamipide to modulate immune responses, may represent a new therapeutic approach to the clinical management of sicca syndrome in SS patients without producing any side effects.

Rebamipide treatment clearly inhibited the production of serum autoantibodies, IgM, and IgG1 and induced a reduction in the transcriptional activity of IRF-4 via down-regulation of NF-κB. It has been reported that IRF-4 functions redundantly with IRF-8 to regulate B cell differentiation into immature IgM+ B cells (43). IRF-4 has been shown to regulate the induction of BLIMP-1 expression and BLIMP-1–dependent plasma cell differentiation (44). The majority of IgM and IgG1 are autoreactive and are also reactive with DNA, phosphorylcholine, phosphatidylcholine, and α1–3-dextran. The process of autoantibody production in SS is characterized by findings of both an antigen-driven response and a polyclonal B cell activation. The causes of this abnormal activation have not been fully elucidated and are likely to vary in different patients and in different animal models of autoimmune diseases. These diseases are characterized by a high titer of autoantibodies that may play a role in the tissue damage. It is possible that the down-regulatory effect of rebamipide on the immune response would be a good therapeutic approach.

We have previously reported that treatment with anti-CD4 and anti-CD86 mAb, cathepsin S inhibitor, caspase inhibitor, and cyclosporin A improved the autoimmune pathology in this mouse model of SS (11,45–48). In the present study, we observed less drastic effects of rebamipide on histologic features, as compared with those in previous therapeutic experiments. This may be related to the relatively low degree of inhibitory effects on T cell–mediated immune responses. Although we did not simply compare the efficacy of rebamipide with that of systemic administration of a different agent, this successful therapeutic effect of rebamipide would provide the possibility of establishing a new form of therapy for patients with autoimmune symptoms caused by SS as well as other types of diseases.

ACKNOWLEDGMENTS

The authors thank Ai Nagaoka, Hiroyo Amo, and Satoko Yoshida for technical assistance.

AUTHOR CONTRIBUTIONS

Dr. Hayashi had full access to all of the data in the study and takes responsibility for the integrity of the data and the accuracy of the data analysis.

Study design. Kohashi, Ishimaru, Hayashi.
Acquisition of data. Kohashi, Arakaki.
Analysis and interpretation of data. Kohashi.
Manuscript preparation. Kohashi, Ishimaru, Hayashi.
Statistical analysis. Kohashi.

REFERENCES

1. Fox RI. Sjögren's syndrome. Lancet 2005;366:321–31.
2. Fox RI, Stern M, Michelson P. Update in Sjögren syndrome. Curr Opin Rheumatol 2000;12:391–8.
3. Kruize AA, Smeenk RJ, Kater L. Diagnostic criteria and immunopathogenesis of Sjögren's syndrome: implications for therapy. Immunol Today 1995;16:557–9.
4. Sebzda E, Mariathasan S, Ohteki T, Jones R, Bachmann MF, Ohashi PS. Selection of the T cell repertoire. Annu Rev Immunol 1999;17:829–74.
5. Starr TK, Jameson SC, Hogquist KA. Positive and negative selection of T cells. Annu Rev Immunol 2003;21:139–76.
6. Wakeland EK, Liu K, Graham RR, Behrens TW. Delineating the genetic basis of systemic lupus erythematosus. Immunity 2001;15:397–408.
7. Yasutomo K. Pathological lymphocyte activation by defective clearance of self-ligands in systemic lupus erythematosus. Rheumatology (Oxford) 2003;42:214–22.
8. Marrack P, Kappler J, Kotzin BL. Autoimmune disease: why and where it occurs. Nat Med 2001;7:899–905.
9. Davidson A, Diamond B. Autoimmune diseases. N Engl J Med 2001;345:340–50.
10. Yasutomo K, Horiuchi T, Kagami S, Tsukamoto H, Hashimura C, Urushihara M, et al. Mutation of DNASE1 in people with systemic lupus erythematosus. Nat Genet 2001;28:313–4.
11. Saegusa K, Ishimaru N, Yanagi K, Mishima K, Arakaki R, Suda T, et al. Prevention and induction of autoimmune exocrinopathy is dependent on pathogenic autoantigen cleavage in murine Sjögren's syndrome. J Immunol 2002;169:1050–7.
12. Bieganowska KD, Ausubel LJ, Modabber Y, Slovik E, Messersmith W, Hafler DA. Direct ex vivo analysis of activated, Fas-sensitive autoreactive T cells in human autoimmune disease. J Exp Med 1997;185:1585–94.
13. Miranda-Carus ME, Askanase AD, Clancy RM, Di Donato F, Chou TM, Libera MR, et al. Anti-SSA/Ro and anti-SSB/La autoantibodies bind the surface of apoptotic fetal cardiocytes and promote secretion of TNF-α by macrophages. J Immunol 2000;165:5345–51.
14. Avrameas S. Natural autoantibodies: from 'horror autotoxicus' to 'gnothi seauton'. Immunol Today 1991;12:154–9.
15. Toubi E, Etzioni A. Intravenous immunoglobulin in immunodeficiency states: state of the art. Clin Rev Allergy Immunol 2005;29:167–72.
16. Barabas AZ, Cole CD, Barabas AD, Lafreniere R. Production of

a new model of slowly progressive Heymann nephritis. Int J Exp Pathol 2003;84:245–58.
17. Ravetch JV. Fc Receptors. In: Paul WE, editor. Fundamental immunology. 5th ed. Philadelphia: Lippincott Williams & Wilkins; 2003. p. 685–700.
18. McCarthy J, O'Mahony L, O'Callaghan L, Sheil B, Vaughan EE, Fitzsimons N, et al. Double blind, placebo controlled trial of two probiotic strains in interleukin 10 knockout mice and mechanistic link with cytokine balance. Gut 2003;52:975–80.
19. Kishimoto S, Haruma K, Tari A, Sakurai K, Nakano M, Nakagawa Y. Rebamipide, an antiulcer drug, prevents DSS-induced colitis formation in rats. Dig Dis Sci 2000;45:1608–16.
20. Bamba H, Ota S, Kato A, Miyatani H, Kawamoto C, Yoshida Y, et al. Effect of rebamipide on prostaglandin receptors-mediated increase of inflammatory cytokine production by macrophages. Aliment Pharmacol Ther 2003;18 Suppl 1:113–8.
21. Hayashi Y, Kojima A, Hata M, Hirokawa K. A new mutation involving the sublingual gland in NFS/N mice: partially arrested mucous cell differentiation. Am J Pathol 1988;132:187–91.
22. Haneji N, Hamano H, Yanagi K, Hayashi Y. A new animal model for primary Sjögren's syndrome in NFS/sld mutant mice. J Immunol 1994;153:2769–77.
23. Ishimaru N, Saegusa K, Yanagi K, Haneji N, Saito I, Hayashi Y Estrogen deficiency accelerates autoimmune exocrinopathy in murine Sjögren's syndrome through Fas-mediated apoptosis. Am J Pathol 1999;155:173–81.
24. Saito I, Haruta K, Shimuta M, Inoue H, Sakurai H, Yamada K, et al. Fas ligand-mediated exocrinopathy resembling Sjögren's syndrome in mice transgenic for IL-10. J Immunol 1999;162:2488–94.
25. Haneji N, Nakamura T, Takio K, Yanagi K, Higashiyama H, Saito I, et al. Identification of α-fodrin as a candidate autoantigen in primary Sjögren's syndrome. Science 1997;276:604–7.
26. Angelin-Duclos C, Johnson K, Liao J, Lin KI, Calame K. An interfering form of Blimp-1 increases IgM secreting plasma cells and blocks maturation of peripheral B cells. Eur J Immunol 2002;32:3765–75.
27. Dong L, Ito S, Ishii KJ, Klinman DM. Suppressive oligodeoxynucleotides delay the onset of glomerulonephritis and prolong survival in lupus-prone NZB × NZW mice. Arthritis Rheum 2005; 52:651–8.
28. Anderson BE, McNiff J, Yan J, Doyle H, Mamula M, Shlomchik MJ, et al. Memory CD4$^+$ T cells do not induce graft-versus-host disease. J Clin Invest 2003;112:101–8.
29. Amend B, Doster H, Lange C, Dubois E, Kalbacher H, Melms A, et al. Induction of autoimmunity by expansion of autoreactive CD4$^+$CD62L^{low} cells in vivo. J Immunol 2006;177:4384–90.
30. Franceschini F, Cavazzana I. Anti-Ro/SSA and La/SSB antibodies. Autoimmunity 2005;38:55–63.
31. Hayashi Y, Arakaki R, Ishimaru N. Apoptosis and estrogen deficiency in primary Sjögren syndrome [published erratum appears in Curr Opin Rheumatol 2004;16:753]. Curr Opin Rheumatol 2004;16:522–6.
32. Turkcapar N, Olmez U, Tutkak H, Duman M. The importance of α-fodrin antibodies in the diagnosis of Sjögren's syndrome. Rheumatol Int 2006;26:354–9.
33. Chan EK, Hamel JC, Buyon JP, Tan EM. Molecular definition and sequence motifs of the 52-kD component of human SS-A/Ro autoantigen. J Clin Invest 1991;87:68–76.
34. Nepom GT. Therapy of autoimmune diseases: clinical trials and new biologics. Curr Opin Immunol 2002;14:812–5.
35. Peakman M, Dayan CM. Antigen-specific immunotherapy for autoimmune disease: fighting fire with fire? Immunology 2001; 104:361–6.
36. Fox RI, Maruyama T. Pathogenesis and treatment of Sjögren's syndrome. Curr Opin Rheumatol 1997;9:393–9.
37. Hasegawa S, Sekino H, Matsuoka O, Saito K, Sekino H, Morikawa A, et al. Bioequivalence of rebamipide granules and tablets in healthy adult male volunteers. Clin Drug Investig 2003;23:771–9.
38. Matysiak-Budnik T, de Mascarel A, Abely M, Mayo K, Heyman M, Megraud F. Positive effect of rebamipide on gastric permeability in mice after eradication of Helicobacter felis. Scand J Gastroenterol 2000;35:470–5.
39. Matysiak-Budnik T, van Niel G, Megraud F, Mayo K, Bevilacqua C, Gaboriau-Routhiau V, et al. Gastric Helicobacter infection inhibits development of oral tolerance to food antigens in mice. Infect Immun 2003;71:5219–24.
40. Naito Y, Yoshikawa T, Tanigawa T, Sakurai K, Yamasaki K, Uchida M, et al. Hydroxyl radical scavenging by rebamipide and related compounds: electron paramagnetic resonance study. Free Radic Biol Med 1995;18:117–23.
41. Yamasaki K, Kanbe T, Chijiwa T, Ishiyama H, Morita S. Gastric mucosal protection by OPC-12759, a novel antiulcer compound, in the rat. Eur J Pharmacol 1987;142:23–9.
42. Makiyama K, Takeshima F, Kawasaki H, Zea-Iriarte WL. Anti-inflammatory effect of rebamipide enema on proctitis type ulcerative colitis: a novel therapeutic alternative. Am J Gastroenterol 2000;95:1838–9.
43. Lu R, Medina KL, Lancki DW, Singh H. IRF-4,8 orchestrate the pre-B-to-B transition in lymphocyte development. Genes Dev 2003;17:1703–8.
44. Klein U, Casola S, Cattoretti G, Shen Q, Lia M, Mo T, et al. Transcription factor IRF4 controls plasma cell differentiation and class-switch recombination. Nat Immunol 2006;7:773–82.
45. Saegusa K, Ishimaru N, Yanagi K, Haneji N, Nishino M, Azuma M, et al. Treatment with anti-CD86 costimulatory molecule prevents the autoimmune lesions in murine Sjögren's syndrome (SS) through up-regulated Th2 response. Clin Exp Immunol 2000;119: 354–60.
46. Hayashi Y, Ishimaru N, Arakaki R, Tsukumo S, Fukui H, Kishihara K, et al. Effective treatment of a mouse model of Sjögren's syndrome with eyedrop administration of anti-CD4 monoclonal antibody. Arthritis Rheum 2004;50:2903–10.
47. Tsubota K, Saito I, Ishimaru N, Hayashi Y. Use of topical cyclosporin A in a primary Sjögren's syndrome mouse model. Invest Ophthalmol Vis Sci 1998;39:1551–9.
48. Saegusa K, Ishimaru N, Yanagi K, Arakaki R, Ogawa K, Saito I, et al. Cathepsin S inhibitor prevents autoantigen presentation and autoimmunity. J Clin Invest 2002;110:361–9.

Biochemical and Biophysical Research Communications 372 (2008) 395–399

Contents lists available at ScienceDirect

Biochemical and Biophysical Research Communications

journal homepage: www.elsevier.com/locate/ybbrc

Effects of coumestrol on lipid and glucose metabolism as a farnesoid X receptor ligand ☆

Miki Takahashi [a,d], Tomohiko Kanayama [b,d], Takuya Yashiro [b], Hidehiko Kondo [a], Takatoshi Murase [a], Tadashi Hase [a], Ichiro Tokimitsu [a], Jun-ichi Nishikawa [c], Ryuichiro Sato [b,d,*]

[a] Biological Science Laboratories, Kao Corporation, 2606 Akabane, Ichikai-machi, Haga-gun, Tochigi 321-3497, Japan
[b] Department of Applied Biological Chemistry, Graduate School of Agricultural and Life Science, The University of Tokyo, 1-1-1 Yayoi, Bunkyo-ku, Tokyo 113-8657, Japan
[c] School of Pharmacy and Pharmaceutical Sciences, Mukogawa Women's University, 11-68 Kyuban-cho, Koshien, Nishinomiya, Hyogo 663-8179, Japan
[d] Basic Research Activities of Innovative Biosciences, Tokyo 105-0001, Japan

ARTICLE INFO

Article history:
Received 23 April 2008
Available online 5 May 2008

Keywords:
CoA-BAP system
Coumestrol
Farnesoid X receptor
Glucose metabolism
Ligand
Lipid metabolism
Nuclear receptor
SHP

ABSTRACT

In the course of an effort to identify novel agonists of the farnesoid X receptor (FXR), coumestrol was determined to be one such ligand. Reporter and *in vitro* coactivator interaction assays revealed that coumestrol bound and activated FXR. Treatment of Hep G2 cells with coumestrol stimulated the expression of FXR target genes, thereby regulating the expression of target genes of the liver X receptor and hepatocyte nuclear factor-4α. Through these actions, coumestrol is expected to exert beneficial effects on lipid and glucose metabolism.

The farnesoid X receptor (FXR; NR1H4) is a member of a nuclear receptor superfamily expressed predominantly in the intestine, kidney, and liver. Upon activation by bile acids, which are endogenous FXR ligands, FXR regulates the expression of genes involved in bile acid homeostasis, such as cholesterol-7α hydroxylase [1] and ileal bile acid binding protein [2]. The identification of phospholipid transfer protein (PLTP) [3] and apolipoprotein A-I [4] as FXR target genes suggests that FXR also controls triglyceride (TG) metabolism. Recent studies using FXR-deficient mice, in which serum glucose levels are elevated, demonstrated that FXR also has a regulatory role in glucose homeostasis [5]. In addition, FXR activation induces the expression of the small heterodimer partner (SHP; NR0B2) [6,7], which acts as a corepressor for several nuclear receptors, including liver X receptor α (LXRα; NR1H3) and hepatocyte nuclear factor-4α (HNF-4α; NR2A1) [8,9]. LXRα is a sterol-responsive transcription factor that regulates the expression of sterol response element-binding protein 1c (SREBP1c) [10,11], which in turn regulates lipogenic enzymes. The best-characterized HNF-4α target genes are those involved in lipid transport and glucose metabolism. Thus, FXR regulates lipid and glucose metabolism through the FXR-SHP cascade.

In general, nuclear receptors regulate gene expression in response to ligand binding through the direct recruitment of cofactors [12–14]. In the presence of agonists, the receptor binds coactivators (e.g., TIF2), and in turn associates with additional proteins to form a complex that activates transcription [15]. In the ab-

Abbreviations: ABCA1, ATP-binding cassette transporter A1; AP, alkaline phosphatase; apoB, apolipoprotein B; apoC-III, apolipoprotein C-III; BAP, bacterial alkaline phosphatase; CDCA, chenodeoxy cholic acid; CoA-BAP, coactivator-bacterial alkaline phosphatase; DMSO, dimethyl sulfoxide; ELISA, enzyme-linked immunosorbent assay; ER, estrogen receptor; FAS, fatty acid synthase; FXR, farnesoid X receptor; GST, glutathione-*S* transferase; HNF-4α, hepatocyte nuclear factor-4 α; LBD, ligand binding domain; LXRα, liver X receptor α; MTP, microsomal triglyceride transfer protein; NID, nuclear receptor interaction domain; NR, nuclear receptor; PEPCK, phosphoenolpyruvate carboxykinase; G6Pase, glucose-6-phosphatase; PLTP, phospholipid transfer protein; RT-PCR, reverse-transcription polymerase chain reaction; SHP, small heterodimer partner; SREBP1c, sterol response element-binding protein 1c; TG, triglyceride.

☆ This work was supported by research grants from the Ministry of Education, Science, Sports, and Culture of Japan and the program for promotion of Basic Research Activities for Innovative Biosciences.

* Corresponding author. Address: Department of Applied Biological Chemistry, Graduate School of Agricultural and Life Science, The University of Tokyo, 1-1-1 Yayoi, Bunkyo-ku, Tokyo 113-8657, Japan. Fax: +81 3 5841 8029.
E-mail address: aroysato@mail.ecc.u-tokyo.ac.jp (R. Sato).

0006-291X/$ - see front matter © 2008 Elsevier Inc. All rights reserved.
doi:10.1016/j.bbrc.2008.04.136

sence of agonists, nuclear receptors bind corepressors (e.g., NCoR) and form a complex that represses transcription [16]. The coactivator-bacterial alkaline phosphatase (CoA-BAP) system developed by Kanayama et al. is a new cell-free assay system for evaluating ligand activity that is based on the ligand-dependent interactions between nuclear receptors and cofactors [17]. Using this system to screen food compounds and their derivatives, we determined that coumestrol is a potent FXR agonist. We show here that coumestrol activates FXR, and thereby regulates the expression of genes involved in lipid and glucose metabolism.

Materials and methods

Materials. Coumestrol, chenodeoxy cholic acid (CDCA), and 17-β-estradiol were purchased from Sigma–Aldrich Co. (St. Louis, MO). An FXR ligand, GW4064, was custom synthesized.

CoA-BAP system. LBD protein (ligand binding domain of nuclear receptors) fused to glutathione-*S* transferase (GST) and NID protein (nuclear receptor interaction domain of cofactors) fused to BAP were prepared as described previously [17]. The purified GST-hFXR LBD protein sample, diluted in 0.1 M $NaHCO_3$ (pH 8.4), was incubated on 96-well plates (MaxiSorp; Nalge Nunc Internationals, Roskilde, Denmark). After overnight incubation at 4 °C, excess protein was removed. An appropriate concentration of a test chemical was then added. After 1 h of incubation at 4 °C, excess test chemical was aspirated and purified hTIF2 NID-BAP fusion protein was applied. After 1 h incubation at 4 °C and subsequent washing, *p*-nitrophenyl-phosphoric acid was added to each well as a BAP substrate, and the enzyme reaction was performed at 30 °C. After an appropriate incubation period, the alkaline phosphatase (AP) activity was measured spectrophotometrically at 405 nm on a microtiter plate reader.

Cell culture. The human hepatoma cell line Hep G2 and the embryonic kidney cell line HEK293T were cultured as previously described [18]. The breast cancer cell line MCF-7 was maintained in minimal essential medium (MP Biomedicals, Irvine, CA) supplemented with 10% fetal bovine serum, 2 mmol/l glutamine, 100 U/ml penicillin, 100 μg/ml streptomycin, and 1% non-essential amino acids. Cells were incubated at 37 °C in a humidified atmosphere of 5% CO_2 in air.

Reporter assays. The expression plasmids pGAL4-hFXR and pFLAG-hFXR [19] and reporter plasmid pSHPp-Luc [18] were previously described. HEK293T cells (12-well plate) were transfected with 300 ng of a reporter plasmid (pUAS-Luc or pSHPp-Luc) and 100 ng of a hFXR expression plasmid (pGAL4-hFXR or pFLAG-hFXR), together with 100 ng of a SV40-gal internal control plasmid using the calcium phosphate transfection method. Twenty-four hours after transfection, the cells were treated with test chemicals in minimal essential medium (phenol red free) supplemented with 5% charcoal-stripped fetal bovine serum. After 24 h exposure to the chemicals, luciferase activities were quantified using a Luciferase Assay Systems (Promega, Madison, WI) according to the manufacturer's instructions. β-Galactosidase activity was used as an internal control.

Quantitative reverse transcription-polymerase chain reaction (RT-PCR). Total RNA was extracted from Hep G2 cells or MCF-7 cells using an RNA extraction reagent (ISOGEN; Nippon Gene, Toyama, Japan) and reverse-transcribed using TaqMan reverse transcriptase reagents (Applied Biosystems, Weiterstadt, Germany). Fluorescent real-time PCR was performed using SYBR green PCR master mix on an ABI 7700 system. The sequences of the primers used for quantitative RT-PCR are shown in Supplementary Information Table 1. The mRNA expression data were normalized to 36B4 mRNA levels. TaqMan Gene Expression Assays were used for pS2/TFF1 (Applied Biosystems).

ApoB ELISA assay. Hep G2 cells were cultured in medium containing 5% lipoprotein-deficient serum and treated with test chemicals for 3d. At 18 h before the end of the 3d treatment, the media were replaced with serum-free media. At the end of the treatment, the media were collected and apoB secretion was measured using an ApoB Microwell ELISA Assay Kit (ALerCHEK Inc., Portland, ME) according to the manufacturer's instructions. ApoB secretion was normalized by cell protein determined using a bicinchoninic acid assay (Pierce Chemical Co., Millford, IL).

Results

Ligand-dependent interaction between nuclear receptor and cofactor

To assess the FXR agonist activity of the test compounds, we used an in vitro coactivator interaction assay, the CoA-BAP system. We confirmed that a natural FXR ligand, CDCA, and a synthetic ligand, GW4064, enhanced the AP activity in a dose-dependent manner. Coumestrol increased the AP activity in the FXR-TIF2 system (Fig. 1). In the absence of FXR LBD (GST alone), there was no apparent increase in the AP activity.

Effects of coumestrol on transcriptional activity of FXR

To investigate the effect of coumestrol on FXR transcriptional activity, we used a GAL4 system using a fusion protein that included a GAL4 DNA-binding domain and a full-length hFXR. Micromolar concentrations of coumestrol increased the reporter activity dose-dependently, while CDCA (100 μM) and GW4064 (0.1 μM) caused approximately 30- and 80-fold inductions, respectively (Fig. 2A).

To further examine the effect of coumestrol on FXR transcriptional activity, a reporter assay was performed using the human SHP promoter-containing reporter gene./The reporter activity was induced by 50 μM coumestrol to 2.0-fold over that in non-treated cells, while CDCA (100 μM) and GW4064 (1 μM) enhanced the reporter activity 4- and 3-fold, respectively (Fig. 2B).

Effects of coumestrol on the expression of genes involved in lipid and glucose metabolism

Although the GAL4 system in Fig. 2A revealed that coumestrol is a less potent ligand than CDCA, another reporter assay in Fig. 2B showed comparable effects between them. To evaluate the effect of coumestrol on lipid and glucose metabolism, we performed

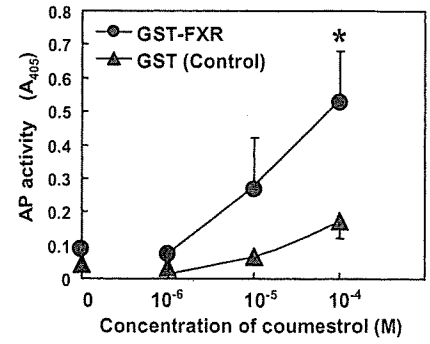

Fig. 1. Assessment of FXR ligand activity using a CoA-BAP system. The CoA-BAP assay was performed with increasing amounts of coumestrol, as described in the Materials and methods. Ligand-dependent interactions between GST-hFXR LBD and hTIF2 NID-BAP were determined as AP activity. AP activity without GST fusion protein was measured as background. Means ± SD ($n = 3$) are shown. $^*P < 0.05$ compared with control (GST alone).

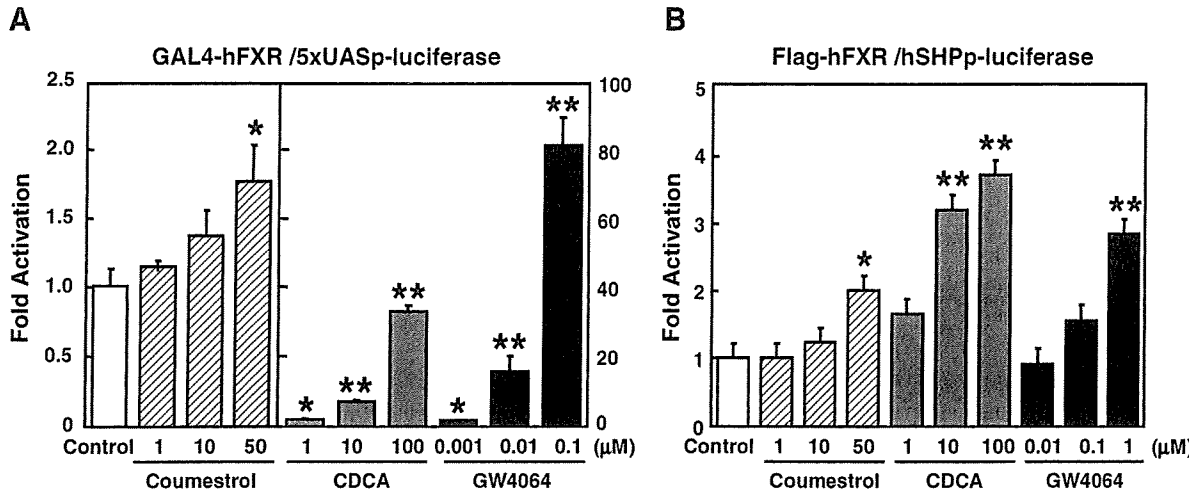

Fig. 2. Coumestrol stimulates FXR transcriptional activity. HEK293T cells were cotransfected with a pGAL4-hFXR expression plasmid and a pUAS-Luc reporter plasmid together with a SV40-gal internal control plasmid and treated for 24 h with coumestrol (1, 10, or 50 μM), CDCA (1, 10, or 100 μM), GW4064 (0.001, 0.01, or 0.1 μM), or DMSO (control) (A). HEK293T cells were cotransfected with a pFLAG-hFXR expression plasmid and a reporter plasmid of SHPp-Luc, together with a SV40-gal internal control plasmid, and treated with coumestrol (1, 10, or 50 μM), CDCA (1, 10, or 100 μM), GW4064 (0.01, 0.1, or 1 μM), or DMSO (control) (B) for 24 h before assaying luciferase activity. Means ± SD ($n = 3$) are shown. $^{*}P < 0.05$, $^{**}P < 0.01$ compared vehicle-treated cells.

quantitative RT-PCR to measure the mRNA levels of metabolism-related genes. The expression levels of FXR target genes, such as SHP and PLTP, were upregulated in Hep G2 cells treated with coumestrol as well as CDCA for 24 h (Fig. 3A), suggesting that the GAL4 system in Fig. 2A underestimated coumestrol functions. Coumestrol treatment decreased the expression of LXR target genes, such as SREBP1c and ATP-binding cassette transporter A1 (ABCA1), SREBP1c target fatty acid synthase (FAS) (Fig. 3B), and HNF-4α target genes, such as microsomal triglyceride transfer protein (MTP), apolipoprotein B (apoB), apolipoprotein C-III (apoC-III), phosphoenolpyruvate carboxykinase (PEPCK), and glucose-6-phosphatase (G6Pase) (Fig. 3C). To exclude the possibility that the upregulation of SHP by coumestrol was accomplished via the estrogen receptor (ER) [20], we evaluated the estrogen responsiveness of Hep G2 cells. In ER-positive MCF-7 cells treated with 10 nM 17-β-estradiol, expression of the ER target gene pS2/TFF1 increased over 14-fold compared to untreated controls, whereas neither pS2/TFF1 nor SHP were induced by 17-β-estradiol in Hep G2 cells (data not shown).

Reduced apolipoprotein B secretion from Hep G2 cells

To examine whether the suppression of MTP and apoB gene expression leads to reduced apoB secretion, we determined the

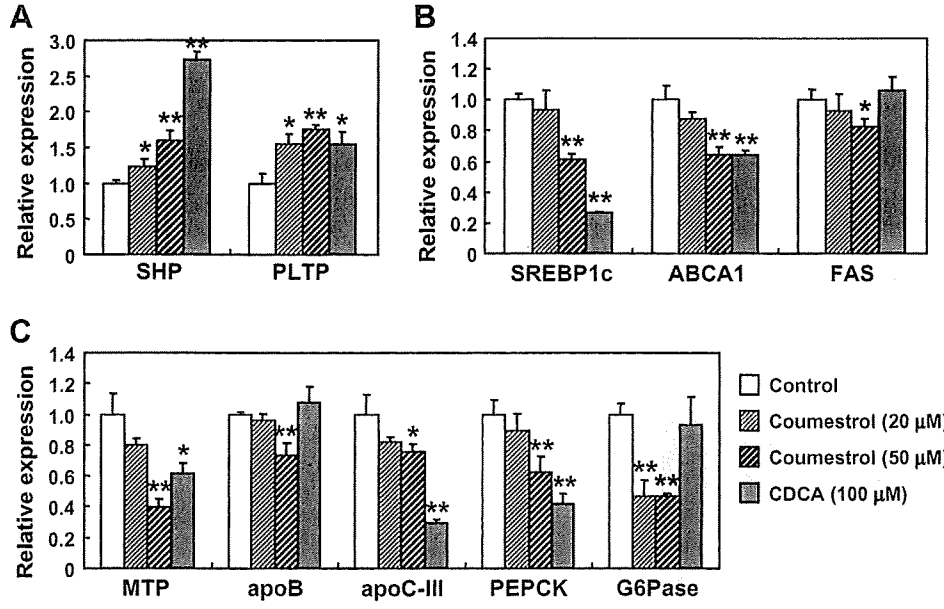

Fig. 3. Coumestrol regulates the expression of genes that are involved in lipid and glucose metabolism. Hep G2 cells were incubated with DMSO (control), coumestrol (20 or 50 μM), or CDCA (100 μM) for 24 h. Hepatic expression levels of FXR target genes (SHP and PLTP) (A), LXR target genes (SREBP1c, ABCA1, and FAS) (B), and HNF-4 target genes (MTP, apoB, apoC-III, PEPCK and G6Pase) (C) were measured using quantitative RT-PCR. Data are presented as the fold-change in gene expression relative to that in DMSO-treated control cells. Means ± SD ($n = 3$) are shown. $^{*}P < 0.05$, $^{**}P < 0.01$ compared with vehicle-treated cells.

levels of apoB secreted in the culture medium of Hep G2 cells incubated with coumestrol. Coumestrol (50 μM) reduced apoB secretion by 50% compared to the control, comparable to the decrease observed with CDCA (Fig. 4). Although CDCA treatment had no significant effect on apoB gene expression (Fig. 3C), it seems likely that MTP activity should be a determinant for apoB-containing lipoprotein secretion.

Discussion

Coumestrol is a coumestan phytoestrogen present in soy sprouts and alfalfa [21]. Previous studies demonstrated that coumestrol binds ERα and ERβ [22], effectively lowers total serum cholesterol in ovariectomized rats [23], and prevents ovariectomy-induced bone loss [24]. These effects of coumestrol are generally considered to be due to its estrogenic activity. ERα directly binds the SHP promoter and enhances transcription [20]. This raises the possibility that coumestrol enhanced SHP gene expression in Hep G2 cells through activation of ERα in Fig. 3. Consistent with the previous finding that Hep G2 cells lack any ER activities [20], 17-β-estradiol stimulated the expression of pS2/TFF1, an ER target gene, only in the ER-positive cell line MCF-7, but not in Hep G2 cells. These findings indicate that coumestrol increases SHP gene expression through the direct activation of FXR.

The present study shows a novel regulatory mechanism by which coumestrol exerts its beneficial effects through FXR activation. Reporter gene and *in vitro* coactivator interaction assays revealed that this compound is a potent FXR agonist, thereby bringing about the increased expression of FXR target genes. The subsequent increase in SHP suppresses the expression of LXR and HNF-4α target genes. At the cellular level, coumestrol decreased apoB secretion, as reflected by the downregulation of MTP and apoB gene expression. These results indicate that coumestrol exerts various effects as a bifunctional ligand via an FXR-mediated pathway as well as through an ER-mediated pathway.

In the current experiments, high levels of coumestrol concentration (~50 μM) were required to exert significant effects resembling endogenous FXR ligand, CDCA (100 μM). However, given that both of them were effective at the comparable concentration, coumestrol is likely to be one of potent FXR ligands. Cholic acid, another endogenous FXR ligand, prevents hepatic TG accumulation, very-low density lipoprotein secretion, and elevated serum TG in mouse models of hypertriglyceridemia [25]. Recent *in vivo* studies also demonstrate that FXR ligands are potentially useful targets for the treatment of cholestatic liver disease [6] and dyslipidemia [26]. Taken together, our findings suggest that coumestrol might improve metabolic disorders such as hypertriglyceridemia, fatty liver disease, and diabetes, at least partly through the activation of FXR.

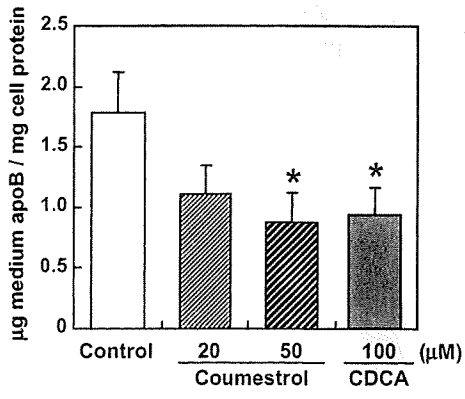

Fig. 4. Coumestrol reduced apoB secretion from Hep G2 cells. Hep G2 cells were cultured in medium containing DMSO (control), coumestrol (20 or 50 μM), or CDCA (100 μM) for 3 d, and apoB secretion into media for the last 18 h was measured using ELISA. Means ± SD ($n = 3$) are shown. $^{*}P < 0.05$ compared with vehicle-treated cells.

A recent report demonstrated that coumestrol functions as a naturally occurring agonist of the pregnane X receptor [27]. In the report, this compound was evaluated as a week agonist of several nuclear receptors including FXR using a GAL4 system that must be a similar system we used. It is possible that coumestrol greatly regulated gene expression of FAS, apoB and G6Pase rather than CDCA (Fig. 3) by taking advantage of the ligand activities of multiple nuclear receptors.

In conclusion, the results of the present study indicate that coumestrol activates FXR and regulates the expression of genes involved in lipid and glucose metabolism, suggesting that coumestrol exerts beneficial effects on metabolic disorders, including hypertriglyceridemia and diabetes. Moreover, the results provide evidence that the CoA-BAP system, in combination with various other analyses, is a practical and useful new strategy for identifying novel bioactive substances.

Appendix A. Supplementary data

Supplementary data associated with this article can be found, in the online version, at doi:10.1016/j.bbrc.2008.04.136.

References

[1] J.Y. Chiang, R. Kimmel, C. Weinberger, D. Stroup, Farnesoid X receptor responds to bile acids and represses cholesterol 7α-hydroxylase gene (CYP7A1) transcription, J. Biol. Chem. 275 (2000) 10918–10924.
[2] J. Grober, I. Zaghini, H. Fujii, S.A. Jones, S.A. Kliewer, T.M. Willson, T. Ono, P. Besnard, Identification of a bile acid-responsive element in the human ileal bile acid-binding protein gene. Involvement of the farnesoid X receptor/9-cis-retinoic acid receptor heterodimer, J. Biol. Chem. 274 (1999) 29749–29754.
[3] N.L. Urizar, D.H. Dowhan, D.D. Moore, The farnesoid X-activated receptor mediates bile acid activation of phospholipid transfer protein gene expression, J. Biol. Chem. 275 (2000) 39313–39317.
[4] T. Claudel, E. Sturm, H. Duez, I.P. Torra, A. Sirvent, V. Kosykh, J.C. Fruchart, J. Dallongeville, D.W. Hum, F. Kuipers, B. Staels, Bile acid-activated nuclear receptor FXR suppresses apolipoprotein A-I transcription via a negative FXR response element, J. Clin. Invest. 109 (2002) 961–971.
[5] K. Ma, P.K. Saha, L. Chan, D.D. Moore, Farnesoid X receptor is essential for normal glucose homeostasis, J. Clin. Invest. 116 (2006) 1102–1109.
[6] B. Goodwin, S.A. Jones, R.R. Price, M.A. Watson, D.D. McKee, L.B. Moore, C. Galardi, J.G. Wilson, M.C. Lewis, M.E. Roth, P.R. Maloney, T.M. Willson, S.A. Kliewer, A regulatory cascade of the nuclear receptors FXR, SHP-1 and LRH-1 represses bile acid biosynthesis, Mol. Cell 6 (2000) 517–526.
[7] T.T. Lu, M. Makishima, J.J. Repa, K. Schoonjans, T.A. Kerr, J. Auwerx, D.J. Mangelsdorf, Molecular basis for feedback regulation of bile acid synthesis by nuclear receptors, Mol. Cell 6 (2000) 507–515.
[8] Y.K. Lee, H. Dell, D.H. Dowhan, M. Hadzopoulou-Cladaras, D.D. Moore, The orphan nuclear receptor SHP inhibits hepatocyte nuclear factor 4 and retinoid X receptor transactivation: two mechanisms for repression, Mol. Cell. Biol. 20 (2000) 187–195.
[9] C. Brendel, K. Schoonjans, O.A. Botrugno, E. Treuter, J. Auwerx, The small heterodimer partner interacts with the liver X receptor α and represses its transcriptional activity, Mol. Endocrinol. 16 (2002) 2065–2076.
[10] J.J. Repa, G. Liang, J. Ou, Y. Bashmakov, J.M. Lobaccaro, I. Shimomura, B. Shan, M.S. Brown, J.L. Goldstein, D.J. Mangelsdorf, Regulation of mouse sterol regulatory element-binding protein-1c gene (SREBP-1c) by oxysterol receptors, LXRα and LXRβ, Genes Dev. 14 (2000) 2819–2830.
[11] T. Yoshikawa, H. Shimano, M. Amemiya-Kudo, N. Yahagi, A.H. Hasty, T. Matsuzaka, H. Okazaki, Y. Tamura, Y. Iizuka, K. Ohashi, J. Osuga, K. Harada, T. Gotoda, S. Kimura, S. Ishibashi, N. Yamada, Identification of liver X receptor-retinoid X receptor as an activator of the sterol regulatory element-binding protein 1c gene promoter, Mol. Cell. Biol. 21 (2001) 2991–3000.
[12] N.J. McKenna, R.B. Lanz, B.W. O'Malley, Nuclear receptor coregulators: cellular and molecular biology, Endocr. Rev. 20 (1999) 321–344.
[13] T.N. Collingwood, F.D. Urnov, A.P. Wolffe, Nuclear receptors: coactivators, corepressors and chromatin remodeling in the control of transcription, J. Mol. Endocrinol. 23 (1999) 255–275.
[14] D. Robyr, A.P. Wolffe, W. Wahli, Nuclear hormone receptor coregulators in action: diversity for shared tasks, Mol. Endocrinol. 14 (2000) 329–347.
[15] J.J. Voegel, M.J. Heine, C. Zechel, P. Chambon, H. Gronemeyer, TIF2, a 160 kDa transcriptional mediator for the ligand-dependent activation function AF-2 of nuclear receptors, EMBO J. 15 (1996) 3667–3675.

[16] J.D. Chen, R.M. Evans, A transcriptional co-repressor that interacts with nuclear hormone receptors, Nature 377 (1995) 454–457.
[17] T. Kanayama, S. Mamiya, T. Nishihara, J. Nishikawa, Basis of a high-throughput method for nuclear receptor ligands, J. Biochem. (Tokyo) 133 (2003) 791–797.
[18] T. Kanayama, M. Arito, K. So, S. Hachimura, J. Inoue, R. Sato, Interaction between sterol regulatory element-binding proteins and liver receptor homolog-1 reciprocally suppresses their transcriptional activities, J. Biol. Chem. 282 (2007) 10290–10298.
[19] M. Nakahara, N. Furuya, K. Takagaki, T. Sugaya, K. Hirota, A. Fukamizu, T. Kanda, H. F ujii, R. Sato, Ileal bile acid-binding protein, functionally associated with the farnesoid X receptor or the ileal bile acid transporter, regulates bile acid activity in the small intestine, J. Biol. Chem. 280 (2005) 42283–42289.
[20] K. Lai, D.C. Harnish, M.J. Evans, Estrogen receptor α regulates expression of the orphan receptor small heterodimer partner, J. Biol. Chem. 278 (2003) 36418–36429.
[21] B.E. Knuckles, D. De Fremery, G.O. Kohler, Coumestrol content of fractions obtained during wet processing of alfalfa, J. Agr. Food Chem. 24 (1976) 1177–1180.
[22] G.G. Kuiper, B. Carlsson, K. Grandien, E. Enmark, J. Haggblad, S. Hilsson, J.A. Gustafsson, Comparison of the ligand binding specificity and transcript tissue distribution of estrogen receptors α and β, Endocrinology 138 (1997) 863–870.
[23] J.A. Dodge, A.L. Glasebrook, D.E. Magee, D.L. Phillips, M. Sato, L.L. Short, H.U. Bryant, Environmental estrogens: effects on cholesterol lowering and bone in the ovariectomized rat, J. Steroid Biochem. Mol. Biol. 59 (1996) 155–161.
[24] C.R. Draper, M.J. Edel, I.M. Dick, A.G. Randall, G.B. Martin, R.L. Prince, Phytoestrogens reduce bone loss and bone resorption in oophorectomized rats, J. Nutr. 127 (1997) 1795–1799.
[25] M. Watanabe, S.M. Houten, L. Wang, A. Moschetta, D.J. Mangelsdorf, R.A. Heyman, D.D. Moore, J. Auwerx, Bile acids lower triglyceride levels via a pathway involving FXR, SHP, and SREBP-1c, J. Clin. Invest. 113 (2004) 1408–1418.
[26] N.L. Urizar, A.B. Liverman, D.T. Dodds, F.V. Silva, P. Ordentlich, Y.Z. Yan, F.J. Gonzalez, R.A. Heyman, D.J. Mangelsdorf, D.D. Moore, A natural product that lowers cholesterol as an antagonist ligand for FXR, Science 296 (2002) 1703–1706.
[27] H. Wang, H. Li, L.B. Moore, M.D. Johnson, J.M. Maglich, B. Goodwin, O.R. Ittoop, B. Wisely, K. Creech, D.J. Parks, J.L. Collins, T.M. Willson, G.V. Kalpana, M. Venkatesh, W. Xie, S.Y. Cho, J. Roboz, M. Redinbo, J.T. Moore, S. Mani, The phytoestrogen coumestrol is a naturally occurring antagonist of the human pregnane X receptor, Mol. Endocrinol. 22 (2008) 838–857.

Published November 24, 2008

ARTICLE

Expression of the retinoblastoma protein RbAp48 in exocrine glands leads to Sjögren's syndrome–like autoimmune exocrinopathy

Naozumi Ishimaru,[1] Rieko Arakaki,[1] Satoko Yoshida,[1] Akiko Yamada,[1] Sumihare Noji,[2] and Yoshio Hayashi[1]

[1]Department of Oral Molecular Pathology, Institute of Health Biosciences, [2]Department of Life Systems, Institute of Technology and Science, The University of Tokushima Graduate School, Tokushima 770-8504, Japan

Although several autoimmune diseases are known to develop in postmenopausal women, the mechanisms by which estrogen deficiency influences autoimmunity remain unclear. Recently, we found that retinoblastoma-associated protein 48 (RbAp48) induces tissue-specific apoptosis in the exocrine glands depending on the level of estrogen deficiency. In this study, we report that transgenic (Tg) expression of RbAp48 resulted in the development of autoimmune exocrinopathy resembling Sjögren's syndrome. CD4$^+$ T cell–mediated autoimmune lesions were aggravated with age, in association with autoantibody productions. Surprisingly, we obtained evidence that salivary and lacrimal epithelial cells can produce interferon-γ (IFN-γ) in addition to interleukin-18, which activates IFN regulatory factor-1 and class II transactivator. Indeed, autoimmune lesions in *Rag2*$^{-/-}$ mice were induced by the adoptive transfer of lymph node T cells from *RbAp48*-Tg mice. These results indicate a novel immunocompetent role of epithelial cells that can produce IFN-γ, resulting in loss of local tolerance before developing gender-based autoimmunity.

CORRESPONDENCE
Yashio Hayashi:
hayashi@dent.tokushima-u.ac.jp

Abbreviations used: CIITA, class II transactivator; cLN, cervical LN; HSG, human salivary gland; IRF, IFN regulatory factor; MSG, mouse salivary gland; NOD, nonobese diabetic; RA, rheumatoid arthritis; RbAp48, retinoblastoma-associated protein 48; SLE, systemic lupus erythematosus; SS, Sjögren's syndrome; Tg, transgenic.

Autoimmune disease is controlled by environments that include gene variants or various cytokines (1, 2). It can increase susceptibility to autoimmunity by affecting the overall reactivity and quality of the cells of the immune system. There is an autoimmune disease specific for certain organs in the body, involving a response to an antigen expressed only in those organs. Antigen/organ specificity is affected by antigen presentation and recognition, antigen expression, and the state and response of the target organs (3, 4), which are maintained by a local immune system termed here "local tolerance."

Many mechanisms protect tissues from autoimmune damage. These include relative isolation from the immune system and inhibition of the function of invading lymphocytes. For example, the eye has barriers to T cell infiltration and produces immunosuppressive cytokines, such as TGF-β (5). Constitutive expression of Fas ligand within the privileged site might also prevent immune-mediated damage by eliminating Fas-expressing T cells (6). Although they have yet to be well demonstrated in spontaneous animal models or human disease, genetic effects at the level of tissue protection are therefore to be expected. Autoimmune organ damage can be mediated by CD4$^+$ T cells, which play a crucial role in the development of autoimmunity (7–9). MHC class II alleles are probably involved in autoimmune disease because different alleles have different abilities to present peptides from target cells to autoreactive CD4$^+$ T cells (10, 11). Certain class II alleles might predispose to autoimmunity by increasing positive selection or decreasing negative selection of autoreactive T cells in the thymus. They might also act by inhibiting selection in the thymus of the regulatory CD4$^+$ T cells that are thought to prevent autoantigen-specific responses. Evidence for the local tolerance hypothesis is provided by the observation that

N. Ishimura and R. Arakaki contributed equally to this paper.
The online version of this article contains supplemental material.

The Rockefeller University Press $30.00
J. Exp. Med. Vol. 205 No. 12 2915-2927
www.jem.org/cgi/doi/10.1084/jem.20080174

Supplemental Material can be found at:
http://jem.rupress.org/content/suppl/2008/11/17/jem.20080174.DC1.html

Published November 24, 2008

autoimmune diseases are often tissue specific and sometimes involve antibodies against a restricted set of antigens, thereby prompting us to accept this most simple explanation for the initiation of autoimmunity. The loss of local tolerance is considered to result from the combined effect of different environmental factors. MHC class II genes are constitutively expressed only on hematopoietic cells involved in antigen presentation (dendritic cells, macrophages, B cells, and cortical thymic epithelial cells), but can be aberrantly induced by inflammatory stimuli on many other cell types (such as endothelial cells, hepatocytes, β cells of the pancreas, and thyrocytes) (12, 13). Although it has been implicated in allograft rejection (14), and subsequently in autoimmunity, it is still unknown whether to initiate autoimmunity class II molecules have to be expressed on professional APCs within secondary lymphoid organs or on nonhematopoietic cells of the target organ itself.

It has been suggested that estrogenic action is responsible for the strong female preponderance of many autoimmune diseases, including systemic lupus erythematosus (SLE), rheumatoid arthritis (RA), and Sjögren's syndrome (SS) (15, 16). Recent evidence suggests that apoptosis plays a key role in the physiology and pathogenesis of various autoimmune diseases, including SS (17–21). We have demonstrated that estrogenic action influences target epithelial cells through Fas-mediated apoptosis in a murine model for SS (21). Recently, we found that tissue-specific apoptosis in the exocrine glands spontaneously occurring in estrogen-deficient mice may contribute to the development of autoimmune exocrinopathy (22). Searching for the role of estrogen deficiency in the development of autoimmunity, we have recently identified retinoblastoma-associated protein 48 (RbAp48) gene specific for estrogen deficiency–dependent apoptosis in the exocrine glands, and transgenic expression of RbAp48 gene induced tissue-specific apoptosis in the exocrine glands (23). In this transgenic mouse model, we propose a possible clear and defined ab initio relationship between aberrant exposure of MHC class II molecules on IFN-γ–producing epithelial cells and disease development (i.e., autoimmune exocrinopathy).

RESULTS

Autoimmune exocrinopathy develops in *RbAp48*-transgenic (Tg) mice

We have generated *RbAp48*-Tg mice where the RbAp48 gene is expressed in the salivary and lacrimal glands using the salivary gland–specific promoter (23). When the histopathology of all organs from those mice were analyzed, we found that autoimmune exocrinopathy resembling SS developed in almost all *RbAp48*-Tg mice at 24 wk of age or more, but not in the WT mice. Lymphocyte infiltration in salivary and lacrimal glands of *RbAp48*-Tg mice becomes more frequent at ~30–50 wk of age (Fig. 1 A), and a significantly higher incidence of inflammatory lesions was found in female Tg mice at all ages (not depicted). Many infiltrating lymphocytes were observed in periductal areas at moderate (score 2) to severe (score 4) degrees, and shown in focal appearance. Representative histopathological features of the inflammatory lesions in lachrymal and salivary (submandibular) glands from *RbAp48*-Tg mice were shown in Fig. 1 B. No inflammatory lesions were observed in other organs of *RbAp48*-Tg mice. A majority of infiltrating cells in salivary and lacrimal glands were Thy1.2$^+$ CD4$^+$ T cells, whereas a minor proportion of B220$^+$ B cells, CD8$^+$ T cells (Fig. 1 C), and CD11b$^+$ cells (unpublished data) was observed. When the function of lacrimal and salivary glands in *RbAp48*-Tg mice was analyzed, the mean volume of tear and saliva secretion from *RbAp48*-Tg mice was significantly lower than that from the WT group at 30 wk of age or more (Fig. 1 D). Regarding the peripheral T cell phenotype of *RbAp48*-Tg mice, T cell activation markers (CD44^{high}, CD62L^{low}, CD45RB^{low}) were up-regulated on CD4$^+$ T cells in cervical LNs (cLNs) from *RbAp48*-Tg mice, compared with those from WT mice (Fig. 2 A). No significant difference was observed in thymic T cells gated on CD4$^+$CD8$^-$ bearing CD69, CD25, and CD62L^{low} between Tg and WT mice (Fig. S1, available at http://www.jem.org/cgi/content/full/jem.20080174/DC1). As for the phenotype of CD4$^+$CD25$^+$Foxp3$^+$ T reg cells, no difference

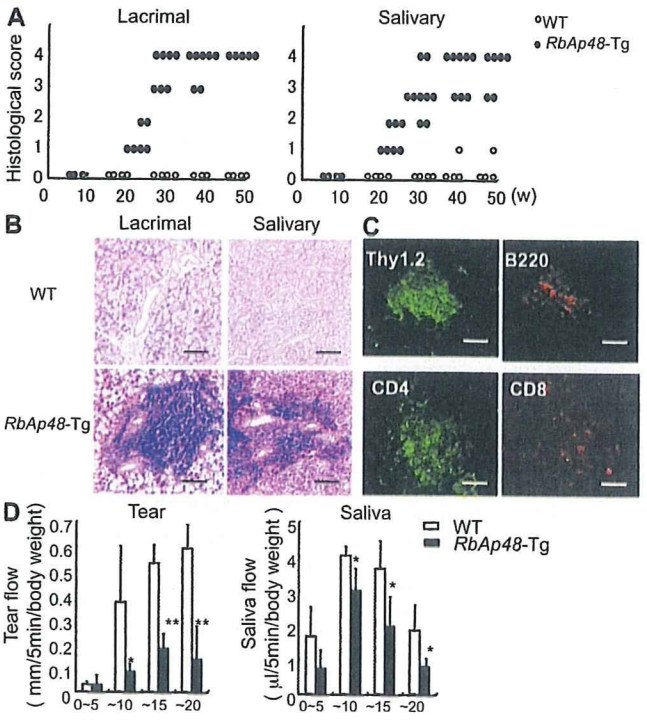

Figure 1. Autoimmune lesions in *RbAp48*-Tg mice. (A) Mean grade of inflammatory lesions in salivary and lacrimal glands from WT and *RbAp48*-Tg mice 10–50 wk of age. (B) Images (H&E staining) are representative of 5–7 mice at 32 wk of age. (C) Lymphocyte populations of the salivary gland lesion from *RbAp48*-Tg mice at 24 wk of age. Thy1.2$^+$, CD4$^+$, CD8$^+$ T cells, or B220$^+$ B cells were detected by immunofluorescence staining with FITC- (green) or PE-conjugated (red) mAbs using the frozen sections. Images are representative of three to five samples from each group. (D) The mean volume of saliva and tear secretion from WT and *RbAp48*-Tg mice at 30 wk of age was measured. Data are means ± SE of five mice. The results are representative of two independent experiments. Bars: (B) 100 μm; (C) 40 μm.

was detected in thymus, spleen, and cLNs between *RbAp48*-Tg and WT mice (Fig. S2). Moreover, culture supernatants from anti–TCR-β and -CD28 mAb-stimulated cLN T cells obtained from *RbAp48*-Tg mice contained higher levels of IL-2 and IFN-γ, whereas no difference in IL-4 and -10 levels between *RbAp48*-Tg and WT mice was observed by ELISA (Fig. 2 B). Our previous reports identified a 120-kD α-fodrin as an important autoantigen in murine and human SS (24, 25). It is particularly interesting that a higher titer of serum autoantibodies against SS-A (Ro), SS-B (La), and 120-kD α-fodrin was detected in *RbAp48*-Tg mice, compared with that in WT mice by ELISA (Fig. 2 C). This result is consistent with the characteristic flow cytometric finding that showed a significant $CD5^+B220^+$ fraction capable of autoantibody production (26) that appeared in spleen cells from *RbAp48*-Tg mice compared with WT mice (Fig. 2 D). On the other hand, the $CD5^+B220^+$ cells were undetectable in both salivary and lacrimal glands from *RbAp48*-Tg mice (Fig. S3 A). In addition, significantly increased $CD21^{high}IgM^{high}B220^+$ marginal zone B cells were observed in both cervical lymph nodes and spleen from *RbAp48*-Tg mice compared with those from WT mice (Fig. S3). These results may provide a new animal model for autoimmune exocrinopathy resembling SS, which should help us to further understand how autoreactive T cells are developed, and subsequently influence the development of autoimmunity.

Salivary gland epithelial cells function as APCs

It is well known that nonlymphoid cells that express MHC class II molecules provoke autoimmune responses (12, 13). However, it is undetermined whether MHC class II–expressing epithelial cells can function as APCs. We frequently observed MHC class II molecule expression on the exocrine gland cells in *RbAp48*-Tg mice, but not in WT mice (Fig. 3 A). These molecules play a pivotal role in the induction and regulation of immune responses by virtue of their ability to present self-peptides to $CD4^+$ T cells (27). To examine whether salivary epithelial cells could act as APCs, mouse salivary gland (MSG) cells, splenocytes, and splenic $CD11c^+$ DCs from *RbAp48*-Tg mice and WT mice were compared in terms of their capacity to express MHC class II and costimulatory molecules, including CD86, CD80, and ICAM-1, by flow cytometric analysis. Among them, a considerably large proportion of MHC class II^+, $CD86^+$ cells, $CD80^+$ cells, and $ICAM\text{-}1^+$ cells was observed on MSG cells from Tg mice, compared with those from WT mice (Fig. 3 B). MSG cells

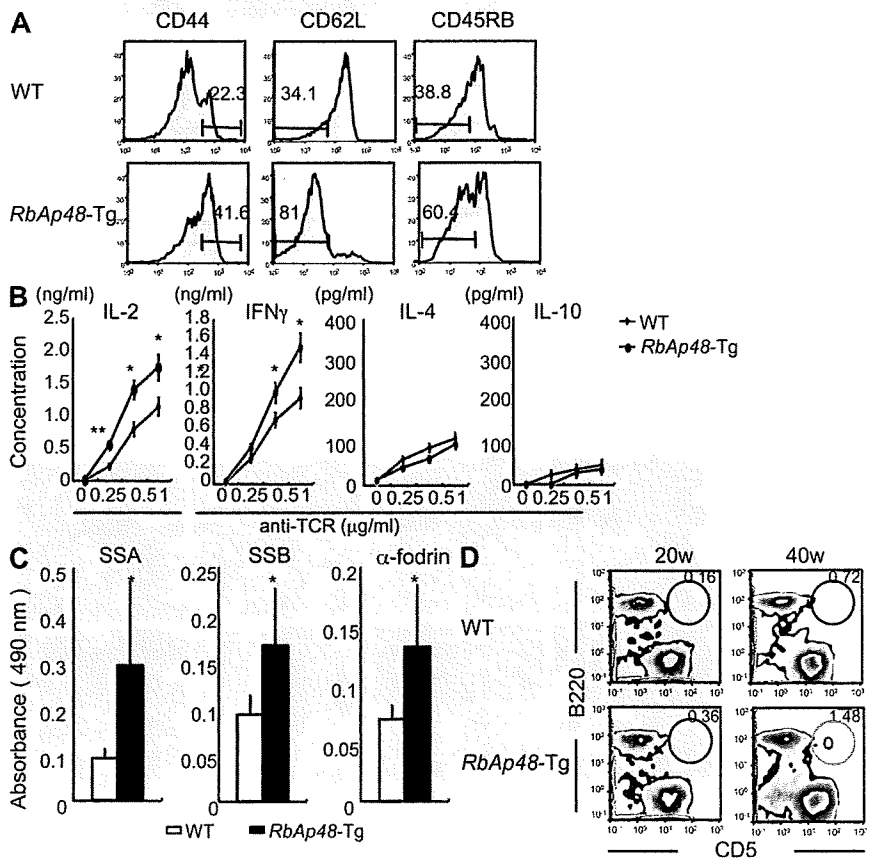

Figure 2. Immune responses in *RbAp48*-Tg mice. (A and B) Activation markers and cytokine production of $CD4^+$ T cells of cLNs from WT and *RbAp48*-Tg mice at 32 wk of age. (C) Autoantibodies of sera from *RbAp48*-Tg mice at 28–32 wk of age. (D) $CD5^+B220^+$ population of spleen from *RbAp48*-Tg and WT mice at 20 and 40 wk of age was analyzed by flow cytometry. Results are representative of means ± SE of five to seven mice in three independent experiments. *, $P < 0.05$; **, $P < 0.005$; WT versus *RbAp48*-Tg mice.

Published November 24, 2008

were enriched by enzymatic treatment and using several antibodies against immune cells, epithelial cells, and magnetic beads, as shown in Fig. S4 A (available at http://www.jem.org/cgi/content/full/jem.20080174/DC1). DCs were undetectable in the purified MSG cell suspension (Fig. S4 B). On the other hand, although the expressions of MHC class II and CD86 on the splenocytes and CD11c$^+$ DCs were higher than those on both MSG cells, the expressions of CD80 and ICAM-1 on the professional APCs were similar or lower than those on the MSG cells (Fig. 3 B). These expressions (MHC class II$^+$, CD86$^+$, CD80$^+$, and ICAM-1$^+$) on salivary epithelial cells from *RbAp48*-Tg mice were also confirmed by confocal analysis (Fig. 3 C). Controls using isotype antibodies for immunostainings were shown in Fig. S4 B. Moreover, to examine whether the peripheral T cells from *RbAp48*-Tg mice can respond to the MSG cells that show phenotypes for the APCs, CFSE-labeled purified CD4$^+$ (10^5) T cells from *RbAp48*-Tg mice were co-cultured with the MSG cells (1 and 2×10^5) from those mice or WT mice. Although CD4$^+$ T cells from B6 mice could not respond to both B6 and *RbAp48*-Tg MSG cells, CD4$^+$ T cells from *RbAp48*-Tg mice were capable of responding to MSG cells from *RbAp48*-Tg mice, but not with those from WT mice, whereas anti–MHC class II antibody inhibits these responses (Fig. 4 A). Furthermore, proliferation assay using [^{3}H]thymidine incorporation demonstrated that purified CD4$^+$ T cells of cLNs from *RbAp48*-Tg mice were more proliferative to the MSG cells from *RbAp48*-Tg mice relative to those from WT mice (Fig. 4 B). Additionally, significantly increased proliferation of the CD4$^+$ T cells to peripheral DCs from *RbAp48*-Tg

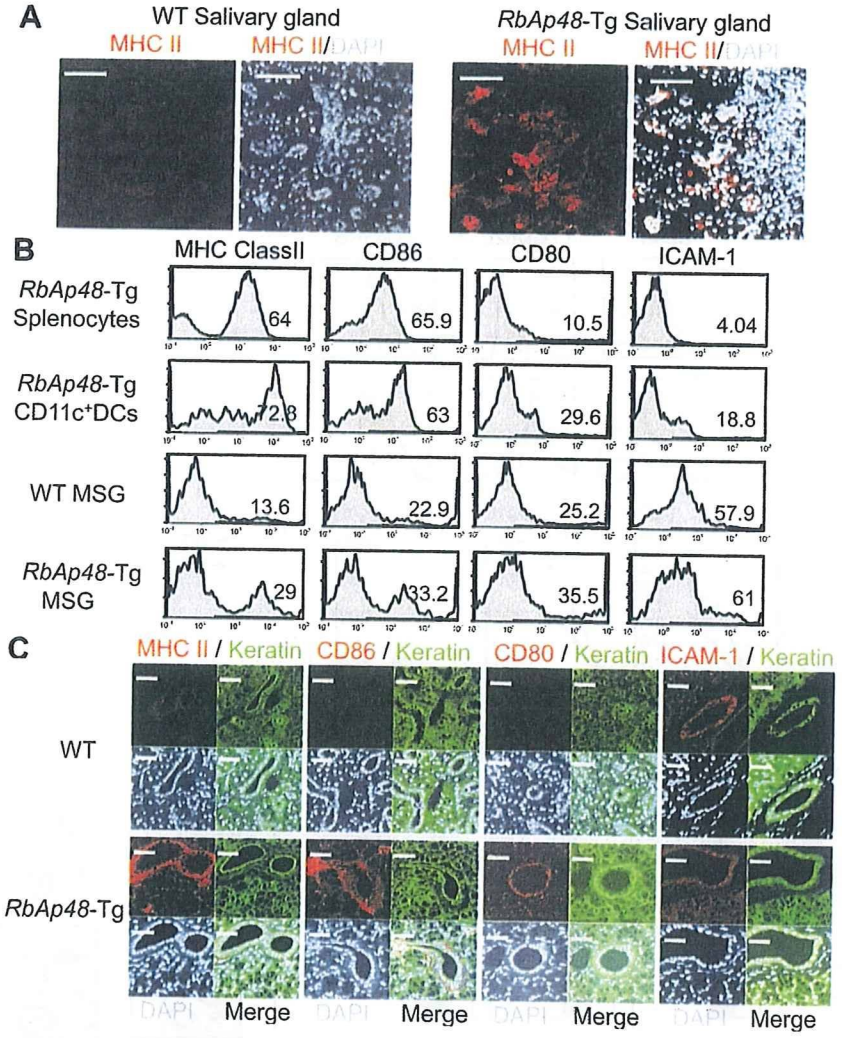

Figure 3. Antigen-presenting function in salivary epithelial cells. (A) MHC class II expression of salivary tissues from WT and *RbAp48*-Tg mice was detected by confocal analysis using anti-MHC class II mAb, Alexa Fluor 568–conjugated anti-rat IgG (red) and DAPI (blue). Images are representative of five to seven mice. (B) APC markers of splenocytes, splenic DCs, and MSG cells from WT and *RbAp48*-Tg mice were analyzed by flow cytometer. Results are representative of three to five mice in two independent experiments. (C) APC markers of MSG epithelial cells were detected by confocal analysis using anti-MHC class II, CD86, CD80, ICAM-1 mAbs, anti-keratin polyclonal antibody, Alexa Fluor 568–conjugated anti-rat IgG (red), Alexa Fluor 488–conjugated anti-rabbit IgG (green), and DAPI (blue). Images are representative of five to seven mice. Bars: (A and C) 50 µm.

mice was observed compared with DCs from WT mice (Fig. 4 C). Approximately half of the T cells response to 10^5 DCs from *RbAp48*-Tg mice equaled the level of the response to 10^5 MSG cells from the Tg mice (Fig. 4, B and C).

Crucial role of epithelial IFN-γ production

The expression of MHC class II molecules is generally regulated at the transcriptional levels, including the transcription factor IFN regulatory factor (IRF)-1 (28, 29) and the class II transactivator (CIITA), which is the master regulator for MHC class II gene expression (30, 31). It has been shown that IRF-1 is a primary responsible gene of the IFN-γ response (32). In in vitro studies using human salivary gland (HSG) cells (33), IFN-γ–induced mRNAs of IRF-1 and CIITA were significantly enhanced by treatment with Tamoxifen (Tam), which is an antagonist of estrogen and can induce RbAp48 (23), or transfection of pCMV-*RbAp48* plasmid in the dose-dependent manner (Fig. 5 A), not in MCF-7 cells (human mammary gland cell line; Fig. S5, A and B, available at http://www.jem.org/cgi/content/full/jem.20080174/DC1). In addition, we next analyzed the IRF-1 promoter activity using *RbAp48*-transfected HSG cells with and without IFN-γ by luciferase assay. We observed significantly enhanced IRF-1 promoter activity in *RbAp48*-transfected HSG cells with IFN-γ, not in MCF-7 cells (Fig. 5 B). Surprisingly, in *RbAp48*-Tg mice, a prominent expression of IFN-γ was detected in salivary and lacrimal epithelial cells besides sporadically positive infiltrating cells of *RbAp48*-Tg mice, not WT mice (Fig. 5 C). These findings were observed mainly in the MHC class II^+ ductal epithelium adjacent to lymphoid infiltrates. Epithelial IFN-γ expression in the exocrine glands of *RbAp48*-Tg mice was up-regulated during the course of autoimmune exocrinopathy. Induction of IFN-γ expression may occur through many different types of stimulation, including cross-linking of cell-surface receptors and stimulation with cytokines, including IL-2, -12, and -18 (34). It has been demonstrated that IFN-γ synthesis is predominantly induced by stimulation with IL-18 (35). Consistent with a previous study (36), IL-18 expression was observed in salivary epithelial cells in *RbAp48*-Tg mice, not in WT mice (Fig. 5 D). Confocal analysis revealed that differential expression of IL-18 and IFN-γ was clearly observed, i.e., IL-18 mainly in the acinar cells and IFN-γ in the duct cells, within salivary epithelial cells from *RbAp48*-Tg mice, but not from WT mice (Fig. 5 D). Controls using isotype antibodies were shown in Fig. S4 C. Epithelial IFN-γ and IL-18 productions were confirmed by flow cytometry using MSG cells without immune cells from *RbAp48*-Tg, not from WT mice, whereas there was no difference in both IFN-γ and IL-18 expressions of cLN cells between WT and *RbAp48*-Tg mice (Fig. 5 E). Although the production of IL-18 in salivary gland cells was detected in a previous study (36), there has been no proof for IFN-γ production of salivary gland cells in any paper. Therefore, to confirm IFN-γ production of exocrine glands, detection of IFN-γ using tissue homogenates was performed. A high concentration of IFN-γ was detected in the tissue homogenates of lacrimal and salivary glands from *RbAp48*-Tg mice, compared with that from WT mice, by ELISA (Fig. S6 A). Furthermore, the detection of IFN-γ mRNA of MSG cells was performed by in situ hybridization using the RNA probe of mouse IFN-γ gene. A more intense signal for IFN-γ mRNA in duct cells of salivary glands from *RbAp48*-Tg mice was observed compared with that from WT mice (Fig. 5 F). As for the expression of BAFF, which is an inducer of IFN-γ in B cells, the expression of epithelial cells was undetectable in both *RbAp48*-Tg and WT mice (Fig. S7). In vitro studies using HSG cells demonstrated that the expressions of IL-18, IFN-γ, and MHC class II (HLA-DR) were observed

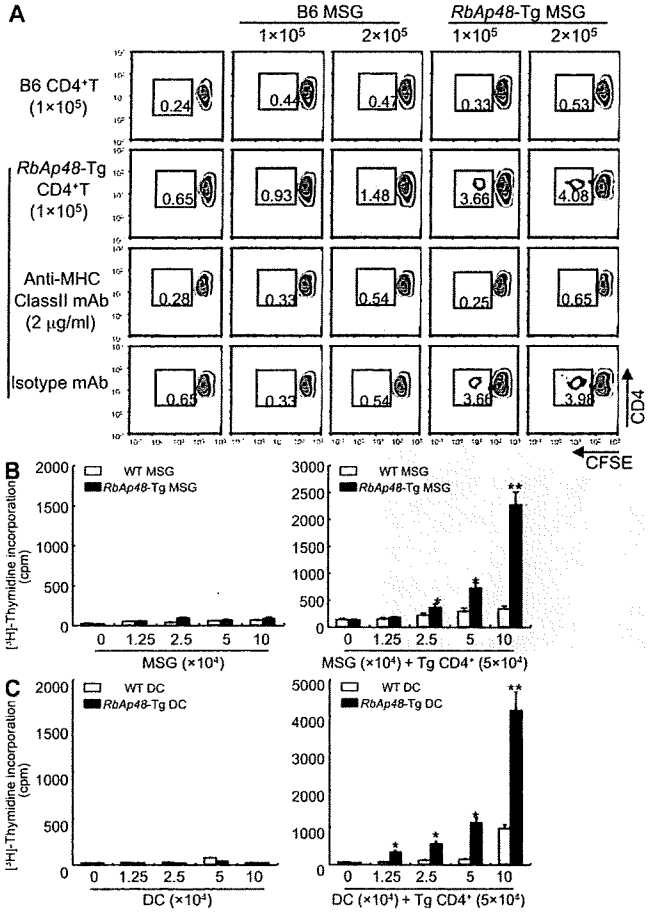

Figure 4. CD4⁺ T cells can proliferate to epithelial cells from *RbAp48*-Tg mice. (A) CFSE-labeled purified CD4⁺ T cells (10^5) of WT and *RbAp48*-Tg mice were co-cultured with MSG cells (1 and 2 × 10^5) from the mice for 72 h. Cell proliferation was estimated by the dilution of CFSE. 2 μg/ml anti-MHC class II mAb or isotype control antibody was added in the culture. All results are representative of three to five mice at 28 wk of age, or three-independent experiments. (B) CD4⁺ T cells (5 × 10^4) of cLNs from *RbAp48*-Tg mice were co-cultured with irradiated MSG cells (0–10 × 10^4) from WT and *RbAp48*-Tg mice for 72 h. (C) CD4⁺ T cells (5 × 10^4) of cLNs from *RbAp48*-Tg mice were co-cultured with irradiated DCs (0–10 × 10^4) from WT and *RbAp48*-Tg mice for 72 h. Proliferative T cell response was evaluated by [³H]thymidine incorporation during the last 12 h of the culture. Results are representative of means ± SE of triplicates in two independent experiments. *, $P < 0.05$; **, $P < 0.005$; WT versus *RbAp48*-Tg MSG cells or DCs.

Published November 24, 2008

when treated with Tam or transfected with pCMV-*RbAp48*, whereas they were inhibited when treated with 17β-estradiol (E2), caspase 1 inhibitor (Ac-YVAD-CHO; Ci), and siRNA of *RbAp48* (si; Fig. 6 A). Confocal analysis confirmed the expression of IL-18 and IFN-γ in HSG cells treated with Tam or transfected with pCMV-*RbAp48* (Fig. 6 B). It is important to note that IL-18 is secreted earlier (by 6 h) than IFN-γ production and HLA-DR expression (by 12 h) in Tam-stimulated and *RbAp48*-transfected HSG cells (Fig. S8). The most prominent function of IL-18 is its capacity to act as a potent costimulus for IFN-γ production (37–39). Indeed, we observed an increase in IFN-γ production in HSG cells treated with

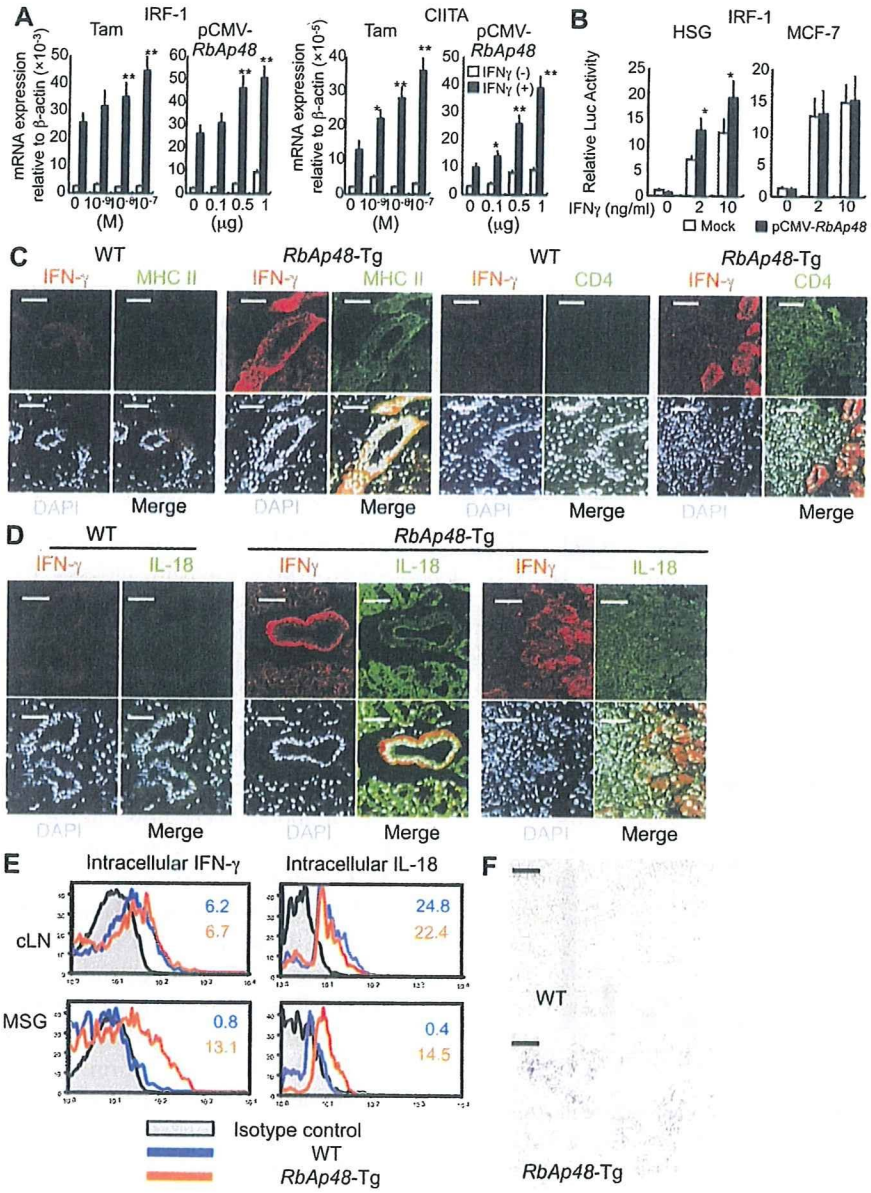

Figure 5. IFN-γ production from salivary epithelial cells stimulated with RbAp48. (A) IRF-1 and CIITA mRNA expressions of HSG cells stimulated with Tam (~10^{-9}–10^{-7} M) or transfected with pCMV-*RbAp48* (~0–1 μg) in the presence of IFN-γ (5 ng/ml) were detected by real-time PCR. Data are shown as means ± SE (SE) relative to β-actin mRNA of two independent experiments. *, $P < 0.05$; **, $P < 0.005$, versus IFN-γ (+) Tam 0 M or IFN-γ (+) pCMV-RbAp48 0 μg. (B) Promoter activity of IRF-1 in HSG and MCF-7 cells transfected with pCMV-*RbAp48*. Data are shown as means ± SE (SE) of two independent experiments. *, $P < 0.05$; **, $P < 0.005$, versus Mock (C and D) Confocal analysis of IFN-γ, MHC Class II, CD4, IL-18 or DAPI of salivary gland tissues from WT and *RbAp48*-TG mice at 32 wk of age. Alexa Fluor 488– or Alexa Fluor 568–conjugated anti-rat IgG were used as the second antibodies. Images are representative of three to five mice. (E) Intracellular IFN-γ and IL-18 expressions of cLN and MSG (without immune cells) cells from WT and *RbAp48*-Tg mice at 32 wk of age was detected by flow cytometric analysis. Results are representative and are shown as means ± SE of three mice of each group in two independent experiments. (F) The expression of IFN-γ mRNA in salivary gland cells of *RbAp48*-Tg mice was detected by in situ hybridization. Representative images of WT and *RbAp48*-Tg mice are shown in two independent experiments. Negative (antisense probe) or positive controls for mouse IFN-γ RNA probe are shown in Fig. S6 B. Fig. S6 is available at http://www.jem.org/cgi/content/full/jem.20080174/DC1. Bars: (C) 50 μm; (D) 40 μm.

Published November 24, 2008

recombinant IL-18 in the dose-dependent manner, but not in MCF-7 cells (Fig. S9, available at http://www.jem.org/cgi/content/full/jem.20080174/DC1), by ELISA and flow cytometry (Fig. 6 C). Confocal analysis of IFN-γ production of HSG cells in response to IL-18 together with cytokeratin as an identified marker was shown in Fig. 6 D. Moreover, we found a significant up-regulation of caspase 1 activity in lacrimal and salivary glands from *RbAp48*-Tg mice relative to that from WT mice (Fig. 6 E). In this regard, we reported previously significantly increased caspase 1 activity in salivary gland tissues from ovariectomized (Ovx) C57BL/6 mice in vivo (22) and Tam-stimulated and *RbAp48*-transfected HSG cells in vitro (23).

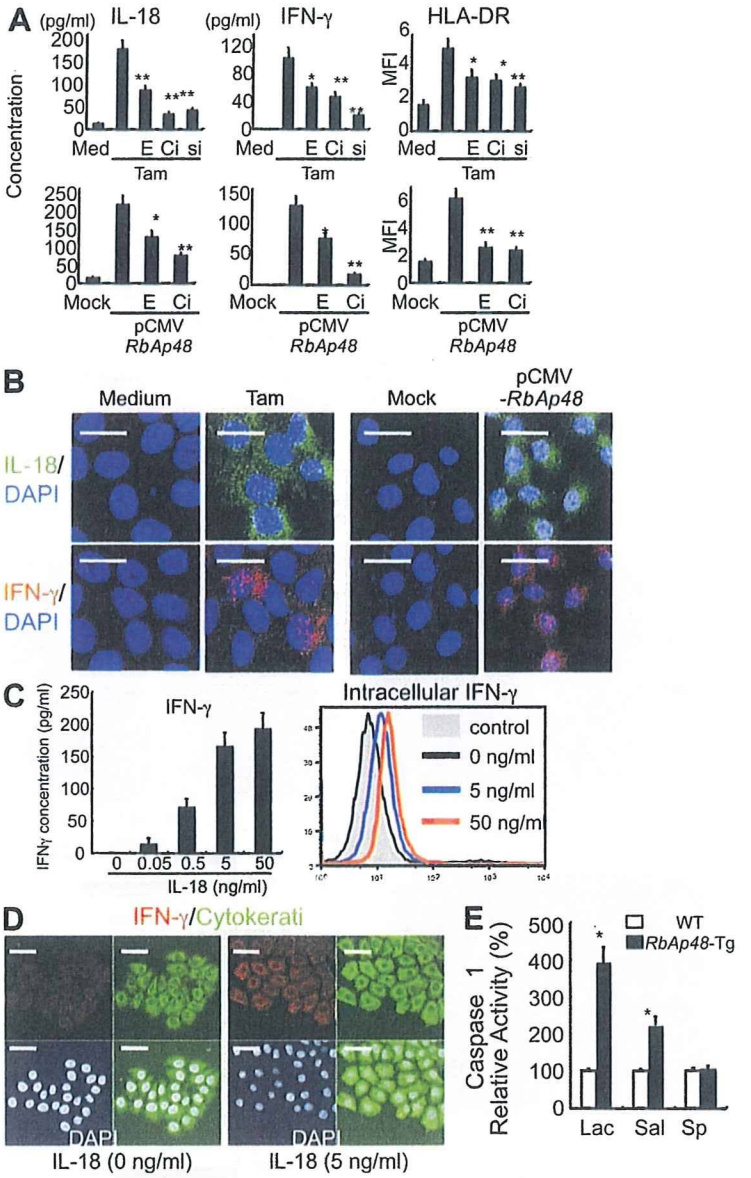

Figure 6. Expressions of IL-18, IFN-γ, and MHC class II (HLA-DR) in HSG cells when treated with Tam and transfected with pCMV-*RbAp48*. (A) Inhibitory effects of 10^{-9} M 17β-estradiol (E) or 10 μM caspase 1 inhibitor (Ci) on RbAp48-induced IL-18, IFN-γ, and HLA-DR in HSG cells. IL-18 and IFN-γ of the culture supernatants were detected by ELISA. HLA-DR is shown as mean fluorescence intensity (MFI) by flow cytometric analysis. *, $P < 0.05$; **, $P < 0.005$, versus RbAp48-induced. Data are means ± SD of triplicate samples, and representative of two independent experiments. (B) Tam- or RbAp48-induced IL-18 and IFN-γ were detected by confocal microscopic analysis. IL-18, IFN-γ mAbs, and Alexa Fluor 488– or Alexa Fluor 568–conjugated anti-mouse IgG were used. Images are representative of three independent experiments. (C) IFN-γ secretion or production of HSG cells by the addition of recombinant IL-18 was detected by ELISA or intracellular flow cytometric analysis. Data are representative of three independent experiments. (D) IFN-γ expression of IL-18–stimulated HSG cells was detected by confocal microscopic analysis together with cytokeratin and DAPI stainings. Images are representative of three independent experiments. (E) Caspase 1 activity of lacrimal, salivary glands, and spleen from *RbAp48*-Tg mice at 28 wk of age. Data are shown as means ± SE of four mice in two independent experiments, relative to those of WT mice. *, $P < 0.05$; **, $P < 0.005$; WT versus *RbAp48*-Tg mice. Bars: (B) 20 μm; (D) 50 μm.

Published November 24, 2008

Transfer of autoimmune exocrinopathy in *RbAp48*-Tg mice

Because thymic T cell abnormality could not be observed in *RbAp48*-Tg mice, it is speculated that there may be dysregulation of peripheral tolerance. To know the homeostatic expansion of peripheral T cells from *RbAp48*-Tg mice, we adoptively transferred CFSE-labeled $CD4^+$ T cells from *RbAp48*-Tg mice into irradiated syngeneic C57BL/6.Ly5.1 mice and analyzed them 7 d later. As a result, we observed more substantial cell division of the donor CFSE-labeled cLN $CD4^+$ T cells from *RbAp48*-Tg mice than that from WT mice (Fig. 7 A), indicating that T cells undergoing homeostatic proliferation may provide a basis for autoimmunity (40, 41). This suggests that elicitation of $CD4^+$ T cell–mediated autoreactivity against autoantigen could be the primary pathogenic process that leads to substantial homeostatic expansion. Futhermore, we succeeded in adoptive transfer of autoimmune lesions in the exocrine glands into *Rag2*$^{-/-}$ mice using cervical lymph node cells, but not spleen cells, from *RbAp48*-Tg mice (Fig. 7, B and C). Interestingly, these transferred lesions were extremely enhanced in estrogen-deficient *Rag2*$^{-/-}$ mice treated with ovariectomy (Ovx) compared with the lesions in Sham *Rag2*$^{-/-}$ mice (Fig. 7, D and F), suggesting that estrogen deficiency accelerates autoimmune exocrinopathy, as previously reported (21, 22). When we examined the adoptive

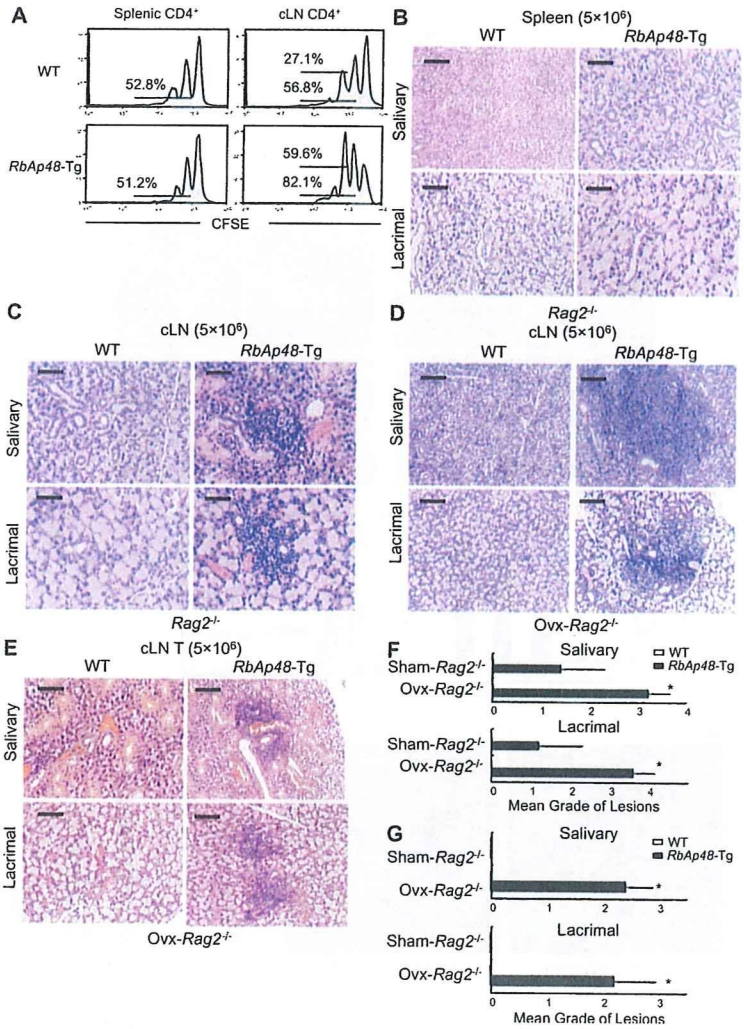

Figure 7. Transfer of autoimmune lesions from *RbAp48*-Tg mice into *Rag2*$^{-/-}$ mice. (A) Homeostatic proliferation of splenic and cLN T cells from WT and *RbAp48*-Tg mice at 28 wk of age was analyzed at 7 d after transfer into irradiated C57BL/6 mice. Results are representative of four to five mice in two independent experiments. Percentages of divided cells from the second or third division are indicated. (B and C) Spleen cells (5×10^6) or cLN cells (5×10^6) from WT and *RbAp48*-Tg mice at 30 wk of age were transferred into *Rag2*$^{-/-}$ mice. At 6 wk after the transfer, the pathology of salivary and lacrimal glands was analyzed. Images are representative of four to five mice. (D) cLN cells from WT and *RbAp48*-Tg mice were transferred into ovariectomized (Ovx) *Rag2*$^{-/-}$ mice. (E) T cells of cLNs from WT and *RbAp48*-Tg mice were transferred into ovariectomized (Ovx) *Rag2*$^{-/-}$ mice. Images of salivary and lacrimal gland tissues were representative of four to five mice. (F) Severity of inflammatory lesions of salivary and lacrimal glands from sham-operated (Sham) and Ovx-*Rag2*$^{-/-}$ hosts by transfer of cLN cells were shown as mean grade of lesions. (G) Severity of inflammatory lesions of salivary and lacrimal glands from sham-operated (Sham) and Ovx-*Rag2*$^{-/-}$ hosts by T cell transfer were shown as mean grade of lesions. Data are shown as means ± SE of four to five mice. *, $P < 0.05$, Sham versus Ovx. Bars: (B–E) 100 µm.